



**DISCRETE AND CONTINUOUS MODELS
AND APPLIED COMPUTATIONAL
SCIENCE**

Volume 27 Number 1 (2019)

Founded in 1993

Founder: PEOPLES' FRIENDSHIP UNIVERSITY OF RUSSIA

DOI: 10.22363/2658-4670-2019-27-1

Edition registered by the Federal Service for Supervision of Communications,
Information Technology and Mass Media

Registration Certificate: ПИ № ФС 77-76317, 19.07.2019

ISSN 2658-7149 (online); 2658-4670 (print)

4 issues per year.

Language: English.

Publisher: Peoples' Friendship University of Russia (RUDN University).

Indexed in Ulrich's Periodicals Directory (<http://www.ulrichsweb.com>),

in Russian Science Citation Index (<https://elibrary.ru>), EBSCOhost

(<https://www.ebsco.com>), CyberLeninka (<https://cyberleninka.ru>).

Aim and Scope

Discrete and Continuous Models and Applied Computational Science arose in 2019 as a continuation of RUDN Journal of Mathematics, Information Sciences and Physics. RUDN Journal of Mathematics, Information Sciences and Physics arose in 2006 as a merger and continuation of the series "Physics", "Mathematics", "Applied Mathematics and Computer Science", "Applied Mathematics and Computer Mathematics".

Discussed issues affecting modern problems of physics, mathematics, queuing theory, the Teletraffic theory, computer science, software and databases development.

It's an international journal regarding both the editorial board and contributing authors as well as research and topics of publications. Its authors are leading researchers possessing PhD and PhDr degrees, and PhD and MA students from Russia and abroad. Articles are indexed in the Russian and foreign databases. Each paper is reviewed by at least two reviewers, the composition of which includes PhDs, are well known in their circles. Author's part of the magazine includes both young scientists, graduate students and talented students, who publish their works, and famous giants of world science.

The Journal is published in accordance with the policies of COPE (Committee on Publication Ethics). The editors are open to thematic issue initiatives with guest editors. Further information regarding notes for contributors, subscription, and back volumes is available at <http://journals.rudn.ru/miph>.

E-mail: miphj@rudn.ru, dcm@sci.pfu.edu.ru.

EDITORIAL BOARD

Editor-in-Chief

Yury P. Rybakov — Doctor of Physical and Mathematical Sciences, professor, Honored Scientist of Russia, professor of the Institute of Physical Research & Technologies, Peoples' Friendship University of Russia (RUDN University), Russian Federation, rybakov-yup@rudn.ru

Vice Editor-in-Chief

Leonid A. Sevastianov — Doctor of Physical and Mathematical Sciences, professor, professor of the Department of Applied Probability and Informatics, Peoples' Friendship University of Russia (RUDN University), Russian Federation, sevastianov-la@rudn.ru

Members of the editorial board

Yu. V. Gaidamaka (Russian Federation) — Doctor of Physical and Mathematical Sciences, associate professor of the Department of Applied Probability and Informatics of Peoples' Friendship University of Russia (RUDN University)

V. I. Il'gisonis (Russian Federation) — Doctor of Physical and Mathematical Sciences, professor, Head of the Institute of Physical Research & Technologies of Peoples' Friendship University of Russia (RUDN University), Head of the direction of scientific and technical research and development of the State Atomic Energy Corporation ROSATOM

K. E. Samouylov (Russian Federation) — Doctor of Engineering Sciences, professor, Head of Department of Applied Probability and Informatics of Peoples' Friendship University of Russia (RUDN University)

Mikhal Hnatich (Slovakia) — DrSc., professor of Pavol Jozef Safarik University in Košice

Datta Gupta Subhashish (India) — PhD in Physics and Mathematics, professor of Hyderabad University

Martikainen, Olli Erkki (Finland) — PhD in Engineering, member of the Research Institute of the Finnish Economy (ETLA, Helsinki)

M. V. Medvedev (USA) — Doctor of Physical and Mathematical Sciences, professor of the Kansas University

Raphael Orlando Ramírez Inostroza (Spain) — PhD professor of Rovira i Virgili University (Universitat Rovira i Virgili), Spain

Bijan Saha (Bangladesh) — Doctor of Physical and Mathematical Sciences, leading researcher in Laboratory of Information Technologies of the Joint Institute for Nuclear Research (Dubna, Russian Federation)

Ochbadrah Chuluunbaatar (Mongolia) — Doctor of Physical and Mathematical Sciences, leading researcher in the Institute of Mathematics, State University of Mongolia, Head of the Department in Laboratory of Information Technologies of the Joint Institute for Nuclear Research (Dubna, Russian Federation)

Computer Design: *A. V. Korolkova*

Address of editorial board:

Ordzhonikidze str., 3, Moscow, Russia, 115419

Tel. +7 (495) 955-07-16, e-mail: publishing@rudn.ru

Editorial office:

Tel. +7 (495) 952-02-50, mipjh@rudn.ru, dcm@sci.pfu.edu.ru

site: <http://journals.rudn.ru/miph>

Paper size 70×100/16. Offset paper. Offset printing. Typeface "Computer Modern".

Conventional printed sheet 5,75. Printing run 500 copies. Open price. The order 2.

PEOPLES' FRIENDSHIP UNIVERSITY OF RUSSIA

6 Miklukho-Maklaya str., 117198 Moscow, Russia

Printed at RUDN Publishing House:

3 Ordzhonikidze str., 115419 Moscow, Russia,

Ph. +7 (495) 952-04-41; e-mail: publishing@rudn.ru



Contents

Queuing theory

Anatoly Nazarov, Svetlana Paul, Olga Lizyura , Heavy outgoing call asymptotics for retrial queue with two way communication and multiple types of outgoing calls	5
---	---

Computational modeling and simulation

Alexander Ayriyan, Ján Buša Jr. , Parallel algorithm for numerical solution of heat equation in complex cylindrical domain	21
Yu Ying , The symbolic problems associated with Runge–Kutta methods and their solving in Sage	33
Yaroslav Yu. Kuziv , Software for the numerical solution of first-order partial differential equations	42

Mathematical modeling

Nikolay Yu. Kravchenko, Dmitry S. Kulyabov , Mathematical model of cavitation under the influence of a single stretching pulse . .	49
Pavel G. Akishin, Andrey A. Sapozhnikov , The volume integral equation method in magnetostatic problem	60



Queuing theory

Research article

UDC 519.872

DOI: 10.22363/2658-4670-2019-27-1-5-20

Heavy outgoing call asymptotics for retrial queue with two way communication and multiple types of outgoing calls

Anatoly Nazarov, Svetlana Paul, Olga Lizyura

*Institute of Applied Mathematics and Computer Science
National Research Tomsk State University
36 Lenina ave., Tomsk, 634050, Russian Federation*

(received: December 7, 2018; accepted: October 21, 2019)

In this paper, we consider a single server queueing model $M|M|1|N$ with two types of calls: incoming calls and outgoing calls, where incoming calls arrive at the server according to a Poisson process. Upon arrival, an incoming call immediately occupies the server if it is idle or joins an orbit if the server is busy. From the orbit, an incoming call retries to occupy the server and behaves the same as a fresh incoming call. The server makes an outgoing calls after an exponentially distributed idle time. It can be interpreted as that outgoing calls arrive at the server according to a Poisson process. There are N types of outgoing calls whose durations follow N distinct exponential distributions. Our contribution is to derive the asymptotics of the number of incoming calls in retrial queue under the conditions of high rates of making outgoing calls and low rates of service time of each type of outgoing calls. Based on the obtained asymptotics, we have built the approximations of the probability distribution of the number of incoming calls in the system.

Key words and phrases: retrial queueing system, incoming calls, outgoing calls, asymptotic analysis method, Gaussian approximation

1. Introduction

Retrial queueing systems are characterized by the following distinctive feature: a customer who cannot receive service remains in the system and tries to occupy the server after some random delay. The pool of unsatisfied customers is called the orbit. Retrial queues have applications in telecommunication, computer networks and in daily life [1, 2].

In retrial queues idle time of the server is the downtime and it should be reduced to increase the efficiency of the system. We consider systems where operator not only receives calls from outside but also makes outgoing calls

© Nazarov A., Paul S., Lizyura O., 2019



This work is licensed under a Creative Commons Attribution 4.0 International License

<http://creativecommons.org/licenses/by/4.0/>

in the idle time. In queueing theory a model with this feature have been considered previously [3]. However, the retrial behaviour of customers is not taken into account. In call centers operators could receive arriving calls but as soon as they have free time and are standby mode they could make outgoing calls [4–7]. Systems with this server behaviour are called retrial queues with two way communication. Retrial Queues with two way communication have been studied recently [8–11]. In these papers Markovian models with two way communication were considered. Model of retrial queue with two way communication and multiple types of outgoing calls was considered by Sakurai and Phung-Duc [12]. For this model numerical algorithm of calculating joint stationary distribution of system state was obtained. Multiserver retrial queue with two way communication was studied in [13]. Recently the two way communication retrial queues with finite source [14], with server-orbit interaction [15, 16], with finite orbit [17], with breakdowns [18] and with a constant retrial rate [19] were considered.

Asymptotic analysis methods have applications in queueing theory. Nazarov, Paul and Gudkova propose an asymptotic analysis method to research $M|M|1|1$ retrial queue with two way communication under low rate of retrials condition [20]. Nazarov, Paul and Phung-Duc extended this model to MMPP $|M|1|1$ retrial queues and derived asymptotics in heavy outgoing call conditions [21].

In this paper, we consider retrial queue with two way communication and multiple types of outgoing calls. We assume that each type of outgoing calls has different rate and service times follow distinct exponential distributions. The main aim of this paper is to derive asymptotics for the model in two limit conditions: i) high rate of outgoing calls and ii) low service rate of outgoing calls. In both cases, the number of incoming calls in the system increases.

The rest of the current paper is organized as follows. In Section 2 and 3, we describe the model in detail and preliminaries for later asymptotic analysis. In Section 4 and 5, we present our main contribution to the model. In Section 6 we show the ranges of parameters under which our approximations are usable. Section 7 is devoted to concluding remarks.

2. Model and preliminaries

2.1. Model description

Figure 1 shows the structure of the model.

We consider a single server retrial queue with two way communication and multiple types of outgoing calls. Incoming calls arrive at the system according to a Poisson process with rate λ and try to occupy the server for an exponentially distributed time with rate μ_1 . Incoming calls that find the server busy join the orbit and repeat their request for service after an exponentially distributed time with rate σ . When the server is idle it makes an outgoing call of type n in an exponentially distributed time with rate α_n . There are N types of outgoing calls whose durations follow N distinct exponential distributions. We assume that the durations of outgoing calls of type n follow the exponential distribution with rate μ_n .

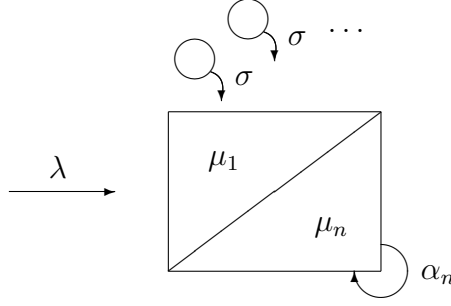


Figure 1. Markovian retrial queue with two way communication and multiple types of outgoing calls

2.2. Problem definition

Let $k(t)$ denote the state of the server at the time $t \geq 0$,

$$k(t) = \begin{cases} 0, & \text{if the server is idle,} \\ 1, & \text{if an incoming call is in service,} \\ n, & \text{if an outgoing call of type } n \text{ is in service, } n = \overline{2, N+1}. \end{cases}$$

Let $i(t)$ denote the number of incoming calls in the system at the time t . It is easy to see that process $\{k(t), i(t)\}$ forms a continuous time Markov chain. We assume that the Markov chain is ergodic and the stationary distribution of $\{k(t), i(t)\}$ exists.

Let $P\{k(t) = k, i(t) = i\} = P_k(i)$ denote the stationary probability distribution of the system state which is the unique solution of Kolmogorov system of equations:

$$\begin{cases} - \left[\lambda + i\sigma + \sum_{n=2}^{N+1} \alpha_n \right] P_0(i) + \mu_1 P_1(i+1) + \sum_{n=2}^{N+1} \mu_n P_n(i) = 0, \\ - (\lambda + \mu_1) P_1(i) + \lambda P_1(i-1) + \lambda P_0(i-1) + i\sigma P_0(i) = 0, \\ - (\lambda + \mu_n) P_n(i) + \lambda P_n(i-1) + \alpha_n P_0(i) = 0, \quad n = \overline{2, N+1}. \end{cases} \quad (1)$$

Let $H_k(u)$ denote the partial characteristic functions $H_k(u) = \sum_{i=0}^{\infty} e^{ju_i} P_k(i)$, $k = \overline{0, N+1}$, where $j = \sqrt{-1}$. Multiplying equations of system (1) by e^{ju_i} and taking the sum over i yields

$$\begin{cases} - \left[\lambda + \sum_{n=2}^{N+1} \alpha_n \right] H_0(u) + j\sigma H'_0(u) + \mu_1 e^{-ju} H_1(u) + \sum_{n=2}^{N+1} \mu_n H_n(u) = 0, \\ - (\lambda + \mu_1) H_1(u) + \lambda e^{ju} H_1(u) + \lambda e^{ju} H_0(u) - j\sigma H'_0(u) = 0, \\ - (\lambda + \mu_n) H_n(u) + \lambda e^{ju} H_n(u) + \alpha_n H_0(u) = 0, \quad n = \overline{2, N+1}. \end{cases} \quad (2)$$

The characteristic function $H(u)$ of the number of incoming calls in the retrial queue is expressed through partial characteristic functions $H_k(u)$ by $H(u) = \sum_{k=0}^{N+1} H_k(u)$. The main content of this paper is the solution of system (2) by using an asymptotic analysis methods in two limit conditions: of the high rate of making outgoing calls and the low rate of service time of outgoing calls.

3. Prelimit analysis

In this section, we obtain expressions for the stationary distribution using the characteristic functions. First, we derive explicit expression for the characteristic function $H(u)$ of the number of incoming calls in the system.

Theorem 1. *Explicit expression for the characteristic function $H(u)$ of the number of incoming calls in $M|M|1|N$ retrial queue is given as follows:*

$$H(u) = \frac{1}{1 + \nu_1} \left(1 + \sum_{n=2}^{N+1} \frac{\alpha_n}{\mu_n + \lambda(1 - e^{ju})} \right) \times \left[\frac{1 - \rho}{1 - \rho e^{ju}} \right]^{\frac{\lambda}{\sigma}(1+\nu_2)+1} \prod_{n=2}^{N+1} \left[\frac{1 - p_n}{1 - p_n e^{ju}} \right]^{\frac{\alpha_n(\theta_n - \lambda)}{\sigma \theta_n}},$$

where

$$\rho = \frac{\lambda}{\mu_1}, \quad \nu_1 = \sum_{k=2}^{N+1} \frac{\alpha_k}{\mu_k}, \quad \nu_2 = \sum_{k=2}^{N+1} \frac{\alpha_k}{\theta_k},$$

$$p_n = \frac{\lambda}{\mu_n + \lambda}, \quad \theta_n = \lambda + \mu_n - \mu_1, \quad n = \overline{2, N+1}.$$

Proof. From equations 2 and 3 of the system (2) we obtain expressions for partial characteristic functions:

$$H_1(u) = \frac{\lambda e^{ju}}{\mu_1 + \lambda(1 - e^{ju})} H_0(u) - \frac{j\sigma}{\mu_1 + \lambda(1 - e^{ju})} H'_0(u), \quad (3)$$

$$H_n(u) = \frac{\alpha_n}{\mu_n + \lambda(1 - e^{ju})} H_0(u), \quad n = \overline{2, N+1}. \quad (4)$$

Substituting this equations into the first equation of the system (2), we find that

$$H'_0(u) = j \frac{\lambda}{\sigma} \left[\frac{\lambda e^{ju}}{\mu_1 - \lambda e^{ju}} + \frac{\mu_1 + \lambda(1 - e^{ju})}{\mu_1 - \lambda e^{ju}} \sum_{n=2}^{N+1} \frac{\alpha_n e^{ju}}{\mu_n + \lambda(1 - e^{ju})} \right] H_0(u). \quad (5)$$

The solution of this differential equation is given by

$$H_0(u) = r_0 \left[\frac{1 - \rho}{1 - \rho e^{ju}} \right]^{\frac{\lambda}{\sigma}(1+\nu_2)} \prod_{n=2}^{N+1} \left[\frac{1 - p_n}{1 - p_n e^{ju}} \right]^{\frac{\alpha_n(\theta_n - \lambda)}{\sigma\theta_n}}, \quad (6)$$

where $\rho = \frac{\lambda}{\mu_1}$, $r_0 = H_0(0) = P\{k(t) = 0\}$, $\nu_2 = \sum_{k=2}^{N+1} \frac{\alpha_k}{\theta_k}$, $p_n = \frac{\lambda}{\mu_n + \lambda}$, $\theta_n = \lambda + \mu_n - \mu_1$, $n = \overline{2, N+1}$.

Substituting $u = 0$ into the system (2) yields:

$$\begin{cases} - \left(\lambda + \sum_{n=2}^{N+1} \alpha_n \right) r_0 + j\sigma H'_0(u)|_{u=0} + \sum_{k=1}^{N+1} \mu_k r_k = 0, \\ - \mu_1 r_1 + \lambda r_0 - j\sigma H'_0(u)|_{u=0} = 0, \\ - \mu_n r_n + \alpha_n r_0 = 0, \quad n = \overline{2, N+1}, \end{cases} \quad (7)$$

where expression for $H'_0(u)|_{u=0}$ can be obtained substituting $u = 0$ into (5).

It follows from equations 2 and 3 of the system (7) that

$$r_1 = \left[\frac{\lambda}{\mu_1} + \frac{\lambda}{\mu_1 - \lambda} \left(\frac{\lambda}{\mu_1} + \sum_{n=2}^{N+1} \frac{\alpha_n}{\mu_n} \right) \right] r_0,$$

$$r_n = \frac{\alpha_n}{\mu_n} r_0, \quad n = \overline{2, N+1}.$$

Furthermore, from the normalization condition: $\sum_{k=0}^{N+1} r_k = 1$, we obtain

$$r_0 = \frac{\mu_1 - \lambda}{\mu_1(1 + \nu_1)}, \quad r_1 = \frac{\lambda}{\mu_1}, \quad r_n = \frac{\alpha_n(\mu_1 - \lambda)}{\mu_1\mu_n(1 + \nu_1)}, \quad n = \overline{2, N+1},$$

where $\nu_1 = \sum_{k=2}^{N+1} \frac{\alpha_k}{\mu_k}$. Substituting (6) into (3) and (4) and summing up results, we obtain

$$H(u) = \frac{1}{1 + \nu_1} \left(1 + \sum_{n=2}^{N+1} \frac{\alpha_n}{\mu_n + \lambda(1 - e^{ju})} \right) \times$$

$$\times \left[\frac{1 - \rho}{1 - \rho e^{ju}} \right]^{\frac{\lambda}{\sigma}(1+\nu_2)+1} \prod_{n=2}^{N+1} \left[\frac{1 - p_n}{1 - p_n e^{ju}} \right]^{\frac{\alpha_n(\theta_n - \lambda)}{\sigma\theta_n}}.$$

4. Asymptotic analysis of the model under the high rate of making outgoing calls

In this section, we will investigate system (2) by asymptotic analysis method under the high rate of making outgoing calls condition. In particular, we prove that asymptotic characteristic function of the number of incoming calls in the system corresponds to Gaussian distribution.

Denoting $\alpha_n = \alpha\gamma_n$, we obtain

$$\begin{cases} - \left[\lambda + \alpha \sum_{n=2}^{N+1} \gamma_n \right] H_0(u) + j\sigma H'_0(u) + \mu_1 e^{-ju} H_1(u) + \sum_{n=2}^{N+1} \mu_n H_n(u) = 0, \\ - (\lambda + \mu_1) H_1(u) + \lambda e^{ju} H_1(u) + \lambda e^{ju} H_0(u) - j\sigma H'_0(u) = 0, \\ - (\lambda + \mu_n) H_n(u) + \lambda e^{ju} H_n(u) + \alpha\gamma_n H_n(u) = 0, \quad n = \overline{2, N+1}. \end{cases} \quad (8)$$

4.1. First order asymptotic

Theorem 2. *Suppose $i(t)$ is the number of incoming calls in the system of the stationary $M|M|1|N$ retrial queue with outgoing calls, then the (9) holds*

$$\lim_{\alpha \rightarrow \infty} E e^{jw \frac{i(t)}{\alpha}} = e^{jw\kappa_1}, \quad (9)$$

where

$$\kappa_1 = \frac{\lambda\nu_1\mu_1}{\sigma(\mu_1 - \lambda)}, \quad \nu_1 = \sum_{n=2}^{N+1} \frac{\gamma_n}{\mu_n}. \quad (10)$$

Proof. We denote $\alpha = 1/\varepsilon$ in the system (8), and introduce the following notations

$$u = \varepsilon w, \quad H_0(u) = \varepsilon F_0(w, \varepsilon), \quad H_k(u) = F_k(w, \varepsilon), \quad k = \overline{1, N+1},$$

in order to get the following system

$$\begin{cases} - (\lambda\varepsilon + \sum_{n=2}^{N+1} \gamma_n) F_0(w, \varepsilon) + j\sigma \frac{\partial F_0(w, \varepsilon)}{\partial w} + \mu_1 e^{-jw\varepsilon} F_1(w, \varepsilon) + \\ \quad + \sum_{n=2}^{N+1} \mu_n F_n(w, \varepsilon) = 0, \\ - (\lambda + \mu_1) F_1(w, \varepsilon) + \lambda e^{jw\varepsilon} F_1(w, \varepsilon) + \lambda e^{jw\varepsilon} \varepsilon F_0(w, \varepsilon) - \\ \quad - j\sigma \frac{\partial F_0(w, \varepsilon)}{\partial w} = 0, \\ - (\lambda + \mu_n) F_n(w, \varepsilon) + \lambda e^{jw\varepsilon} F_n(w, \varepsilon) + \\ \quad + \gamma_n F_0(w, \varepsilon) = 0, \quad n = \overline{2, N+1}. \end{cases} \quad (11)$$

Summing up equations of system (11), we obtain

$$\lambda \varepsilon F_0(w, \varepsilon) + (\lambda - \mu_1 e^{-jw\varepsilon}) F_1(w, \varepsilon) + \lambda \sum_{n=2}^{N+1} F_n(w, \varepsilon) = 0. \quad (12)$$

Considering the limit as $\varepsilon \rightarrow 0$ in the system (11) and equation (12), then we will get

$$\left\{ \begin{array}{l} - \sum_{n=2}^{N+1} \gamma_n F_0(w) + j\sigma F_0'(w) + \sum_{k=1}^{N+1} \mu_k F_k(w) = 0, \\ - \mu_1 F_1(w) - j\sigma F_0'(w) = 0, \\ - \mu_n F_n(w) + \gamma_n F_0(w) = 0, \quad n = \overline{2, N+1}, \\ - (\mu_1 - \lambda) F_1(w) + \lambda \sum_{n=2}^{N+1} F_n(w) = 0. \end{array} \right. \quad (13)$$

We propose to get the solution of the system (13) in the form of

$$F_k(w) = \Phi(w) r_k, \quad k = \overline{0, N+1}. \quad (14)$$

Here r_k , $k = \overline{1, N+1}$ is the probability of the server state k ; r_0 has no sense of probability, since the probability that the server will be in the zero state as $\alpha \rightarrow \infty$ is zero:

$$\left\{ \begin{array}{l} - \sum_{n=2}^{N+1} \gamma_n r_0 + j\sigma \frac{\Phi'(w)}{\Phi(w)} r_0 + \sum_{k=1}^{N+1} \mu_k r_k = 0, \\ - \mu_1 r_1 - j\sigma \frac{\Phi'(w)}{\Phi(w)} r_0 = 0, \\ - \mu_n r_n + \gamma_n r_0 = 0, \quad n = \overline{2, N+1}, \\ - (\mu_1 - \lambda) r_1 + \lambda \sum_{n=2}^{N+1} r_n = 0. \end{array} \right. \quad (15)$$

As the relation $j \frac{\Phi'(w)}{\Phi(w)}$ does not depend on w , the function is obtained in the following form $\Phi(w) = \exp\{jw\kappa_1\}$, which coincides with (9). The value of the parameter κ_1 will be defined below. We rewrite the system (15) in the form

$$\left\{ \begin{array}{l} - \sum_{n=2}^{N+1} \gamma_n r_0 - \kappa_1 r_0 \sigma + \sum_{k=1}^{N+1} \mu_k r_k = 0, \\ - \mu_1 r_1 + \kappa_1 r_0 \sigma = 0, \\ - \mu_n r_n + \gamma_n r_0 = 0, \quad n = \overline{2, N+1}, \\ - (\mu_1 - \lambda) r_1 + \lambda \sum_{n=2}^{N+1} r_n = 0. \end{array} \right. \quad (16)$$

The normalization condition for stationary server state probability distribution is $\sum_{k=1}^{N+1} r_k = 1$. We have

$$\left\{ \begin{array}{l} - \mu_n r_n + \gamma_n r_0 = 0, \quad n = \overline{2, N+1}, \\ - (\mu_1 - \lambda) r_1 + \lambda \sum_{n=2}^{N+1} r_n = 0, \\ \sum_{k=1}^{N+1} r_k = 1. \end{array} \right. \quad (17)$$

The solution of the system (17) is given by

$$r_0 = \frac{\mu_1 - \lambda}{\mu_1 \nu}, \quad r_1 = \frac{\lambda}{\mu_1}, \quad r_n = \frac{\gamma_n (\mu_1 - \lambda)}{\mu_n \mu_1 \nu}, \quad n = \overline{2, N+1}, \quad (18)$$

where $\nu_1 = \sum_{n=2}^{N+1} \frac{\gamma_n}{\mu_n}$. Substituting (18) into system (16), we obtain an equation for κ_1 , which coincides with (10).

The first order asymptotic i.e. Theorem 2, only defines the mean asymptotic value $\kappa_1 \alpha$ of a number of incoming calls in the system in prelimit situation of $\alpha \rightarrow \infty$. For more detailed research of number $i(t)$ of incoming calls in the system let's consider the second order asymptotic. \square

4.2. Second order asymptotic

Theorem 3. *In the context of Theorem 2 the following equation is true*

$$\lim_{\alpha \rightarrow \infty} E \exp \left\{ jw \frac{i(t) - \kappa_1}{\sqrt{\alpha}} \right\} = e^{\frac{(jw)^2}{2} \kappa_2}, \quad (19)$$

where

$$\kappa_2 = \frac{\lambda}{\sigma} \cdot \frac{\mu_1 (\mu_1 - \lambda) (\lambda \nu_2 + \nu_1) + \lambda^2 \nu_1}{(\mu_1 - \lambda)^2}, \quad \nu_1 = \sum_{n=2}^{N+1} \frac{\gamma_n}{\mu_n}, \quad \nu_2 = \sum_{n=2}^{N+1} \frac{\gamma_n}{\mu_n^2}. \quad (20)$$

Proof. We introduce the following notations in the system (8)

$$H_k(u) = \exp\{ju\alpha\kappa_1\}H_k^{(2)}(u), \quad k = \overline{0, N+1}, \quad (21)$$

and we get

$$\left\{ \begin{array}{l} - \left(\lambda + \alpha \sum_{n=2}^{N+1} \gamma_n + \alpha\sigma\kappa_1 \right) H_0^{(2)}(u) + j\sigma \frac{dH_0^{(2)}(u)}{du} + \\ \quad + \mu_1 e^{-ju} H_1^{(2)}(u) + \sum_{n=2}^{N+1} \mu_n H_n^{(2)}(u) = 0, \\ - (\lambda + \mu_1) H_1^{(2)}(u) + \lambda e^{ju} H_1^{(2)}(u) + (\lambda e^{ju} + \alpha\sigma\kappa_1) H_0^{(2)}(u) - \\ \quad - j\sigma \frac{dH_0^{(2)}(u)}{du} = 0, \\ - (\lambda + \mu_n) H_n^{(2)}(u) + \lambda e^{ju} H_n^{(2)}(u) + \\ \quad + \alpha\gamma_n H_0^{(2)}(u) = 0, \quad n = \overline{2, N+1}. \end{array} \right. \quad (22)$$

Denoting $\alpha = 1/\varepsilon^2$, and introducing the following notations

$$\begin{aligned} u &= w\varepsilon, \quad H_0^{(2)}(u) = \varepsilon^2 F_0^{(2)}(w, \varepsilon), \\ H_k^{(2)}(u) &= F_k^{(2)}(w, \varepsilon), \quad k = \overline{1, N+1}, \end{aligned} \quad (23)$$

we obtain

$$\left\{ \begin{array}{l} j\sigma\varepsilon \frac{\partial F_0^{(2)}(w, \varepsilon)}{\partial w} - \left(\sigma\kappa_1 + \lambda\varepsilon^2 + \sum_{n=2}^{N+1} \gamma_n \right) F_0^{(2)}(w, \varepsilon) + \\ \quad + \mu_1 e^{-jw\varepsilon} F_1^{(2)}(w, \varepsilon) + \sum_{n=2}^{N+1} \mu_n F_n^{(2)}(w, \varepsilon) = 0, \\ - (\lambda + \mu_1) F_1^{(2)}(w, \varepsilon) + \lambda e^{jw\varepsilon} F_1^{(2)}(w, \varepsilon) + \\ \quad + (\lambda e^{jw\varepsilon} \varepsilon^2 + \sigma\kappa_1) F_0^{(2)}(w, \varepsilon) - j\sigma\varepsilon \frac{\partial F_0^{(2)}(w, \varepsilon)}{\partial w} = 0, \\ - (\lambda + \mu_n) F_n^{(2)}(w, \varepsilon) + \lambda e^{jw\varepsilon} F_n^{(2)}(w, \varepsilon) + \\ \quad + \gamma_n F_0^{(2)}(w, \varepsilon) = 0, \quad n = \overline{2, N+1}. \end{array} \right. \quad (24)$$

Summing up equations of the system (24), we obtain

$$\lambda\varepsilon^2 F_0^{(2)}(w, \varepsilon) + (\lambda - \mu_1 e^{-jw\varepsilon}) F_1^{(2)}(w, \varepsilon) + \lambda \sum_{n=2}^{N+1} F_n^{(2)}(w, \varepsilon) = 0. \quad (25)$$

Our idea is to seek for a solution of the system (24) and equation (25) in the form

$$F_k^{(2)}(w, \varepsilon) = \Phi_2(w)\{r_k + jw\varepsilon f_k\} + o(\varepsilon^2), \quad k = \overline{0, N+1}. \quad (26)$$

Substituting (26) to (24) and (25), laying out the exhibitors in tailor series and taking (16) into account, dividing these equations by ε and taking the limit as $\varepsilon \rightarrow 0$, we have

$$\begin{aligned} - \left(\sigma\kappa_1 + \sum_{n=2}^{N+1} \gamma_n \right) f_0 + \sum_{k=1}^{N+1} \mu_k f_k - \mu_1 r_1 + \sigma \frac{\Phi_2'(w)}{w\Phi_2(w)} r_0 &= 0, \\ \sigma\kappa_1 f_0 - \mu_1 f_1 + \lambda r_1 - \sigma \frac{\Phi_2'(w)}{w\Phi_2(w)} r_0 &= 0, \\ -\mu_n f_n + \lambda r_n + \gamma_n f_0 &= 0, \quad n = \overline{2, N+1}, \\ -(\mu_1 - \lambda) f_1 + \lambda \sum_{n=2}^{N+1} f_n + \mu_1 r_1 &= 0. \end{aligned}$$

This equations imply that $\frac{\Phi_2'(w)}{w\Phi_2(w)}$ doesn't depend on w and thus the function $\Phi_2(w)$ is given in the following form

$$\Phi_2(w) = \exp \left\{ \frac{(jw)^2}{2} \kappa_2 \right\},$$

which coincides with (19). We have

$$\frac{\Phi_2'(w)}{w\Phi_2(w)} = -\kappa_2$$

and then we obtain the system

$$\begin{cases} - \left(\sigma\kappa_1 + \sum_{n=2}^{N+1} \gamma_n \right) f_0 + \sum_{k=1}^{N+1} \mu_k f_k = \mu_1 r_1 + \sigma\kappa_2 r_0, \\ \sigma\kappa_1 f_0 - \mu_1 f_1 = -\lambda r_1 - \sigma\kappa_2 r_0, \\ -\mu_n f_n + \gamma_n f_0 = -\lambda r_n, \quad n = \overline{2, N+1}, \\ -(\mu_1 - \lambda) f_1 + \lambda \sum_{n=2}^{N+1} f_n = -\mu_1 r_1. \end{cases} \quad (27)$$

Substituting values (18) into the system (27), we have

$$f_n = \frac{\gamma_n}{\mu_n} f_0 + \frac{\lambda(\mu_1 - \lambda)\gamma_n}{\mu_1 \mu_n^2 \nu_1}, \quad n = \overline{2, N+1},$$

$$f_1 = \frac{\lambda\nu_1}{\mu_1 - \lambda} f_0 + \frac{\lambda^2\nu_2}{\mu_1\nu_1} + \frac{\lambda}{\mu_1 - \lambda},$$

where

$$\nu_1 = \sum_{k=2}^{N+1} \frac{\gamma_k}{\mu_k}, \quad \nu_2 = \sum_{k=2}^{N+1} \frac{\gamma_k}{\mu_k^2}.$$

Substituting these expressions into equation 2 of the system (27), we obtain an equation for κ_1 , which coincides with (20).

Second order asymptotic i.e. Theorem 3, shows that the asymptotic probability distribution of the number $i(t)$ of incoming calls in the system is Gaussian with mean asymptotic $\kappa_1\alpha$ and variance $\kappa_2\alpha$. \square

5. Asymptotic analysis of the model under the low rate of service time of outgoing calls

In this section, we will investigate system (2) by asymptotic analysis method under the low rate of service time of outgoing calls condition.

Denoting $\mu_n = \mu\gamma_n$, we obtain

$$\begin{cases} - \left[\lambda + \sum_{n=2}^{N+1} \alpha_n \right] H_0(u) + j\sigma H_0'(u) + \mu_1 e^{-ju} H_1(u) + \mu \sum_{n=2}^{N+1} \gamma_n H_n(u) = 0, \\ - (\lambda + \mu_1) H_1(u) + \lambda e^{ju} H_1(u) + \lambda e^{ju} H_0(u) - j\sigma H_0'(u) = 0, \\ - (\lambda + \mu\gamma_n) H_n(u) + \lambda e^{ju} H_n(u) + \alpha_n H_n(u) = 0, \quad n = \overline{2, N+1}. \end{cases} \quad (28)$$

Theorem 4. *Suppose $i(t)$ is a number of incoming calls in a system of stationary $M|M|1|N$ retrial queue with two way communication, then the following equation is true*

$$H(u) = \lim_{\mu \rightarrow 0} E e^{jw\mu i(t)} = \frac{1}{\nu_1} \sum_{n=2}^{N+1} \frac{\alpha_n}{\gamma_n - jw\lambda} \prod_{n=2}^{N+1} \left(1 - jw \frac{\lambda}{\gamma_n} \right)^{-\frac{\mu_1 \alpha_n}{\sigma(\mu_1 - \lambda)}}, \quad (29)$$

where $\nu_1 = \sum_{n=2}^{N+1} \frac{\alpha_n}{\gamma_n}$.

Proof. We denote $\mu = \varepsilon$, let's substitute the following in the system (28)

$$u = w\varepsilon, \quad H_0(u) = \varepsilon F_0(w, \varepsilon), \quad H_k(u) = F_k(w, \varepsilon), \quad k = \overline{1, N+1}.$$

We will get the system

$$\left\{ \begin{array}{l} - \left(\lambda + \sum_{n=2}^{N+1} \alpha_n \right) \varepsilon F_0(w, \varepsilon) + j\sigma \frac{\partial F_0(w, \varepsilon)}{\partial w} + \\ \quad + \mu_1 e^{-jw\varepsilon} F_1(w, \varepsilon) + \varepsilon \sum_{n=2}^{N+1} \gamma_n F_n(w, \varepsilon) = 0, \\ - (\lambda + \mu_1) F_1(w, \varepsilon) - j\sigma \frac{\partial F_0(w, \varepsilon)}{\partial w} + \lambda e^{jw\varepsilon} F_1(w, \varepsilon) + \\ \quad + \lambda \varepsilon e^{jw\varepsilon} F_0(w, \varepsilon) = 0, \\ - (\lambda + \varepsilon \gamma_n) F_n(w, \varepsilon) + \lambda e^{jw\varepsilon} F_n(w, \varepsilon) + \\ \quad + \alpha_n \varepsilon F_0(w, \varepsilon) = 0, \quad n = \overline{2, N+1}. \end{array} \right. \quad (30)$$

Considering the limit as $\varepsilon \rightarrow 0$ in the system (30) then we will get

$$-j\sigma F_0'(w) - \mu_1 F_1(w) = 0, \quad j\sigma F_0'(w) + \mu_1 F_1(w) = 0. \quad (31)$$

Summing up equations of the system (30) we have

$$\lambda \varepsilon F_0(w, \varepsilon) + (\lambda - \mu_1 e^{-jw\varepsilon}) F_1(w, \varepsilon) + \lambda \sum_{n=2}^{N+1} \gamma_n F_n(w, \varepsilon) = 0. \quad (32)$$

Laying out the exhibitors in tailor series, dividing equations by ε and taking the limit as $\varepsilon \rightarrow 0$, taking (31) into account, we obtain

$$\begin{aligned} - \left(\lambda + \sum_{n=2}^{N+1} \alpha_n \right) F_0(w) - jw\mu_1 F_1(w) + \sum_{n=2}^{N+1} \gamma_n F_n(w) &= 0, \\ -j\sigma F_0'(w) - \mu_1 F_1(w) &= 0, \\ (\lambda jw - \gamma_n) F_n(w) + \alpha_n F_0(w) &= 0, \quad n = \overline{2, N+1} \\ -(\mu_1 - \lambda) F_1(w) + \lambda \sum_{n=2}^{N+1} F_n(w) &= 0. \end{aligned}$$

From the last system of equations we have

$$F_n(w) = \frac{\alpha_n}{\gamma_n - jw\lambda} F_0(w), \quad (33)$$

$$F_1(w) = \frac{\lambda}{\mu_1 - \lambda} \sum_{n=2}^{N+1} F_n(w). \quad (34)$$

Then

$$F_1(w) = \frac{\lambda}{\mu_1 - \lambda} F_0(w) \sum_{n=2}^{N+1} \frac{\alpha_n}{\gamma_n - jw\lambda}. \quad (35)$$

Substituting (35) into (31), we obtain

$$F_0'(w) = j \frac{\lambda \mu_1}{\sigma(\mu_1 - \lambda)} F_0(w) \sum_{n=2}^{N+1} \frac{\alpha_n}{\gamma_n - jw\lambda}.$$

The solution of differential equation is given by

$$F_0(w) = C \prod_{n=2}^{N+1} \left(1 - jw \frac{\lambda}{\gamma_n} \right)^{-\frac{\mu_1 \alpha_n}{\sigma(\mu_1 - \lambda)}}, \quad (36)$$

where C is an integration constant and its value will be obtained later. We denote asymptotic characteristic function $\sum_{k=1}^{N+1} F_k(w) = \Phi(w)$. Substituting (36) into (33) and (34), we obtain

$$F_1(w) = \frac{\lambda}{\mu_1 - \lambda} \sum_{k=2}^{N+1} \frac{\alpha_k}{\gamma_k - jw\lambda} C \prod_{k=2}^{N+1} \left(1 - jw \frac{\lambda}{\gamma_k} \right)^{-\frac{\mu_1 \alpha_k}{\sigma(\mu_1 - \lambda)}},$$

$$F_n(w) = \frac{\alpha_n}{\gamma_n - jw\lambda} C \prod_{k=2}^{N+1} \left(1 - jw \frac{\lambda}{\gamma_k} \right)^{-\frac{\mu_1 \alpha_k}{\sigma(\mu_1 - \lambda)}}, \quad n = \overline{2, N+1}.$$

Summing up equations, we have

$$\Phi(w) = \frac{\mu_1}{\mu_1 - \lambda} C \prod_{n=2}^{N+1} \left(1 - jw \frac{\lambda}{\gamma_n} \right)^{-\frac{\mu_1 \alpha_n}{\sigma(\mu_1 - \lambda)}} \sum_{n=2}^{N+1} \frac{\alpha_n}{\gamma_n - jw\lambda}.$$

Using condition $\Phi(0) = 1$, we obtain

$$C = \frac{\mu_1 - \lambda}{\mu_1 \nu_1}, \quad \text{where } \nu_1 = \sum_{n=2}^{N+1} \frac{\alpha_n}{\gamma_n}.$$

We obtain the characteristic function (29). □

6. Approximation accuracy

The accuracy of the approximation $P^{(2)}(i)$ is defined by using Kolmogorov range $\Delta_2 = \max_{0 \leq i \leq N} \left| \sum_{\nu=0}^i (P(\nu) - P^{(2)}(\nu)) \right|$, which represents the difference between distributions $P(i)$ and $P^{(2)}(i)$, where $P(i)$ is obtained by using inverse

Fourier transform for the characteristic function of the $M|M|1|N$ retrial queue and the approximation $P^{(2)}(i)$ is given by obtained asymptotics. We consider $N = 3$, $\lambda = 0.2$, $\mu_1 = 1$ and $\sigma = 1$ for Tables 1 and 2.

Table 1

Kolmogorov range, $\mu_2 = 2$, $\mu_3 = 3$, $\mu_4 = 4$, $\gamma_2 = 1$, $\gamma_3 = 2$, $\gamma_4 = 3$

	$\alpha = 3$	$\alpha = 5$	$\alpha = 10$	$\alpha = 50$	$\alpha = 100$
Δ_2	0.066	0.043	0.023	0.01	0.007

Table 2

Kolmogorov range, $\gamma_2 = 2$, $\gamma_3 = 3$, $\gamma_4 = 4$, $\alpha_2 = 1$, $\alpha_3 = 2$, $\alpha_4 = 3$

	$\mu = 0.05$	$\mu = 0.035$	$\mu = 0.02$	$\mu = 0.01$
Δ_2	0.059	0.044	0.026	0.014

7. Conclusions

In this paper, we have considered retrial queue with two way communication with multiple types of outgoing calls. We have found characteristic function of the number of incoming calls in the system. We have found the first and the second order asymptotics of the number of calls in the system under the condition of the high rate of making outgoing calls. Based on the obtained asymptotics we have built the Gaussian approximation of the probability distribution of the number of incoming calls in the system. We have found asymptotic characteristic function of the number of incoming calls in retrial queue under the condition of the low service rate of outgoing calls. In future we plan to consider this retrial queueing system under other asymptotic conditions.

Acknowledgments

This research was financially supported by Russian Foundation for Basic Research (the Agreement number 18-01-00277).

References

1. J. R. Artalejo, A. Gómez-Corral, Retrial queueing systems: a computational approach (2008). doi:10.1007/978-3-540-78725-9.
2. G. Falin, J. G. C. Templeton, Retrial queues, Vol. 75, CRC Press, 1997.
3. G. P. Basharin, K. E. Samuylov, On a single-phase queueing system with two types of requests and relative priority [Ob odnofaznoy sisteme massovogo obsluzhivaniya s dvumya tipami zayavok i otnositel'nyim

- prioritetom], Journal of Academy of Sciences of the USSR. Technical Cybernetics [Izvestiya akademii nauk SSSR. Tekhnicheskaya kibernetika] 3 (1983) 48–56, in Russian.
4. S. Bhulai, G. Koole, A queueing model for call blending in call centers, *IEEE Transactions on Automatic Control* 48 (8) (2003) 1434–1438.
 5. A. Deslauriers, P. L’Ecuyer, J. Pichitlamken, A. Ingolfsson, A. N. Avramidis, Markov chain models of a telephone call center with call blending, *Computers & operations research* 34 (6) (2007) 1616–1645.
 6. L. Brown, N. Gans, A. Mandelbaum, A. Sakov, H. Shen, S. Zeltyn, L. Zhao, Statistical analysis of a telephone call center: a queueing-science perspective, *Journal of the American Statistical Association* 100 (469) (2005) 36–50.
 7. S. Aguir, F. Karaesmen, O. Z. Akşin, F. Chauvet, The impact of retrials on call center performance, *OR Spectrum* 26 (3) (2004) 353–376. doi:10.1007/s00291-004-0165-7.
 8. J. R. Artalejo, T. Phung-Duc, Markovian retrial queues with two way communication, *Journal of Industrial and Management Optimization* 8 (4) (2012) 781–806.
 9. J. R. Artalejo, T. Phung-Duc, Single server retrial queues with two way communication, *Applied Mathematical Modelling* 37 (4) (2013) 1811–1822.
 10. T. Phung-Duc, W. Rogiest, Two way communication retrial queues with balanced call blending, in: *International Conference on Analytical and Stochastic Modeling Techniques and Applications*, Springer, 2012, pp. 16–31. doi:10.1007/978-3-642-30782-9_2.
 11. H. Sakurai, T. Phung-Duc, Scaling limits for single server retrial queues with two-way communication, *Annals of Operations Research* 247 (1) (2016) 229–256. doi:10.1007/s10479-015-1874-9.
 12. H. Sakurai, T. Phung-Duc, Two-way communication retrial queues with multiple types of outgoing calls, *Top* 23 (2) (2015) 466–492. doi:10.1007/s11750-014-0349-5.
 13. T. Phung-Duc, K. Kawanishi, An efficient method for performance analysis of blended call centers with redial, *Asia-Pacific Journal of Operational Research* 31 (02) (2014) 1440008. doi:10.1142/s0217595914400089.
 14. A. Kuki, J. Sztrick, Á. Tóth, T. Bérczes, A contribution to modeling two-way communication with retrial queueing systems, in: *Information Technologies and Mathematical Modelling. Queueing Theory and Applications*, Springer, Cham, 2018, pp. 236–247. doi:10.1007/978-3-319-97595-5_19.
 15. V. Dragieva, T. Phung-Duc, Two-way communication M/M/1 retrial queue with server-orbit interaction, in: *Proceedings of the 11th International Conference on Queueing Theory and Network Applications*, ACM, 2016, p. 11.
 16. V. Dragieva, T. Phung-Duc, Two-way communication M/M/1/1 queue with server-orbit interaction and feedback of outgoing retrial calls, in: *International Conference on Information Technologies and Mathematical Modelling*, Springer, 2017, pp. 243–255. doi:10.1007/978-3-319-68069-9_20.

17. S. Ouazine, K. Abbas, A functional approximation for retrial queues with two way communication, *Annals of Operations Research* 247 (1) (2016) 211–227. doi:10.1007/s10479-015-2083-2.
18. M. S. Kumar, A. Dadlani, K. Kim, Performance analysis of an unreliable M/G/1 retrial queue with two-way communication, Springer, 2018, pp. 1–14. doi:10.1007/s12351-018-0430-1.
19. E. Morozov, T. Phung-Duc, Regenerative analysis of two-way communication orbit-queue with general service time, in: *International Conference on Queueing Theory and Network Applications*, Springer, 2018, pp. 22–32. doi:10.1007/978-3-319-93736-6_2.
20. A. A. Nazarov, S. Paul, I. Gudkova, Asymptotic analysis of Markovian retrial queue with two-way communication under low rate of retrials condition, in: *Proceedings 31st European Conference on Modelling and Simulation*, 2017, pp. 678–693.
21. A. Nazarov, T. Phung-Duc, S. Paul, Heavy outgoing call asymptotics for MMPP/M/1/1 retrial queue with two-way communication, in: *International Conference on Information Technologies and Mathematical Modelling*, Springer, 2017, pp. 28–41. doi:10.1007/978-3-319-68069-9_3.

For citation:

A. Nazarov, S. Paul, O. Lizyura, Heavy outgoing call asymptotics for retrial queue with two way communication and multiple types of outgoing calls, *Discrete and Continuous Models and Applied Computational Science* 27 (1) (2019) 5–20. DOI: 10.22363/2658-4670-2019-27-1-5-20.

Information about the authors:

Anatoly A. Nazarov (Russian Federation) — Professor, Doctor of Technical Sciences, Head of Department of Probability Theory and Mathematical Statistics, Institute of Applied Mathematics and Computer Science, National Research Tomsk State University (e-mail: nazarov.tsu@gmail.com, phone: +7(3822)529599, ORCID: <https://orcid.org/0000-0002-2091-6011>, ResearcherID: O-5862-2014, Scopus Author ID: 7201780364)

Svetlana V. Paul (Russian Federation) — Candidate of Physical and Mathematical Sciences, Assistant Professor of Department of Probability Theory and Mathematical Statistics, Institute of Applied Mathematics and Computer Science, National Research Tomsk State University (e-mail: paulsv82@mail.ru, phone: +7(3822)529599, ORCID: <https://orcid.org/0000-0002-3681-0676>, ResearcherID: E-7860-2017, Scopus Author ID: 57031144200)

Olga D. Lizyura (Russian Federation) — Master's Degree Student of Institute of Applied Mathematics and Computer Science, National Research Tomsk State University (e-mail: oliztsu@mail.ru, phone: +7(999)4996743, ORCID: <https://orcid.org/0000-0003-4463-4876>, ResearcherID: G-7896-2019)

Computational modeling and simulation

Research article

PACS 07.05.Tp, 02.60.Pn, 02.70.Bf
DOI: 10.22363/2658-4670-2019-27-1-21-32

Parallel algorithm for numerical solution of heat equation in complex cylindrical domain

Alexander Ayriyan¹, Ján Buša Jr.^{1,2}

¹ *Laboratory of Information Technologies, JINR, Dubna, Russia*

² *Institute of Experimental Physics, Slovak Academy of Sciences, Košice, Slovakia*

(received: April 6, 2019; accepted: October 21, 2019)

In this article we present a parallel algorithm for simulation of the heat conduction process inside the so-called pulse cryogenic cell. This simulation is important for designing the device for portion injection of working gases into ionization chamber of ion source. The simulation is based on the numerical solving of the quasilinear heat equation with periodic source in a multilayered cylindrical domain. For numerical solution the Alternating Direction Implicit (ADI) method is used. Due to the non-linearity of the heat equation the simple-iteration method has been applied. In order to ensure convergence of the iteration process, the adaptive time-step has been implemented. The parallelization of the calculation has been realized with shared memory application programming interface OpenMP and the performance of the parallel algorithm is in agreement with the case studies in literature.

Key words and phrases: quasilinear heat equation, multilayer cylindrical geometrical structure, pulse periodic source, parallel algorithm, thermal gates

1. Introduction

The purpose of this work is to develop algorithms for simulation of the heat conduction process inside the so-called pulse cryogenic cell [1, 2]. Such simulations are important for designing the cell that implements “the thermal gates” of a portion injection of working gases into the ionization chamber of a multiply charged ion source [3]. While reliable operation of mechanical valves for pulsed injection of gaseous mixtures in the millisecond range at cryogenic temperatures is practically impossible, the use of gas temperature properties at cryogenic temperatures can be a real alternative. Indeed, the vapor pressures of various gases have strong dependency on the temperature [4] in the interval between temperatures of liquid helium 4.2 K and liquid nitrogen

78 K [5], typical temperature terminals in the cryogenic technique used as thermostats with large capacity.

The cryogenic cell is a multilayer cylinder (see Fig. 1) placed inside a vacuum chamber. The thermal process in the cylinder starts by passing an electrical current through its conductive layer. It allows heating the outer layer of the cylinder to upper desired temperature (maximal critical temperature). After switching the current off, the cylinder is let to cool down to lower desired temperature (minimal critical temperature). This process periodically repeats for a given period of time based on the requirements of the experiment. A copper core of the cylinder serves as a cooler for outer layers during and after the heating process. It is connected to a liquid helium temperature terminal. The core is separated by the electrical insulator from the conductive layer. It is made to avoid the flow of the electrical current into the core. The last layer is a thin coating which prevents molecules of working gases from binding to the conductive layer made of graphite.

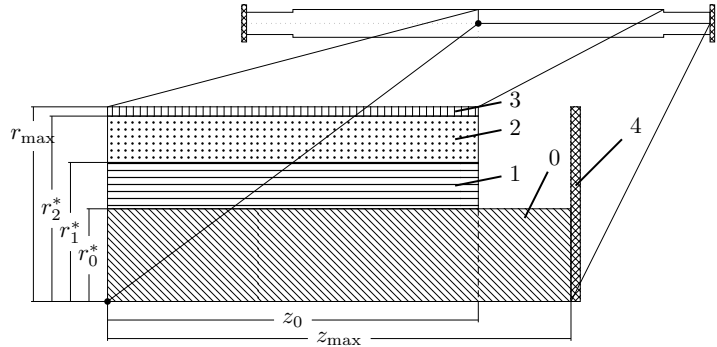


Figure 1. A schematic view of the quarter of the cell slice through the axis. The bottom line is the cylinder axis (the symmetry axis, $r = 0$). The cooler (the copper core rod) cools the cell by contact with the temperature terminal – 4 (liquid helium). The heater – 2 (the conductive layer) heats the cell up by the way of passing of the electrical current. The inner insulator – 1 – is needed to prevent the electrical current outflow from the heater to the cooler. The outer insulator – 3 – prevents molecules of working gases from binding to the conductive layer

2. Initial-boundary value problem

Let us consider the heat equation describing thermal evolution in the closed cylindrical domain $\bar{\Omega} = \{(r, z) \mid r \in [0, r_{\max}(z)], z \in [0, z_{\max}(r)]\}$:

$$\rho(r)c_V(T, r) \frac{\partial T}{\partial t} = \frac{1}{r} \frac{\partial}{\partial r} \left(r \lambda(T, r) \frac{\partial T}{\partial r} \right) + \frac{\partial}{\partial z} \left(\lambda(T, r) \frac{\partial T}{\partial z} \right) + X(T, t, r; t_{\text{per}}, t_{\text{src}}), \quad (1)$$

where the thermal coefficients are the non-linear function of the temperature and they have discontinuities of the first kind along the radial direction at r_m^* ($m = 0, 1, 2, 3$, see Fig. 1). The source function producing the periodic

process of heating can be expressed in the form

$$X(T, t, r; t_{\text{per}}, t_{\text{src}}) = \chi(T) \frac{I^2(r)}{S_C} p(t; t_{\text{per}}, t_{\text{src}}), \quad (2)$$

where $p(t; t_{\text{per}}, t_{\text{src}})$ is the periodic normalized function with parameters t_{per} (time of period) and t_{src} (time of heating less than or equal to t_{per}); $n \in \mathbb{N}_0$ is the index of a period; $\chi(T, r)$ is temperature depended specific resistivity with discontinuities at the given values of r ; $I(r)$ is the electrical current amplitude which has a finite value I_0 only in the source layer (see Fig. 1), everywhere else it is zero; S_C is the cross-section of the source layer. The periodic normalized function $p(t; t_{\text{per}}, t_{\text{src}})$ is given as a rectangular pulse one [6]:

$$u(t; t_{\text{per}}, t_{\text{src}}) = \sum_{n=0}^{\infty} [\theta(t - n t_{\text{per}}) - \theta(t - n t_{\text{per}} - t_{\text{src}})], \quad (3)$$

where $\theta(t)$ is Heaviside step function [7, 8], however, in order to make the processes of “turn on” and “turn off” more realistic, the model of the transient process (4) (see Fig. 2) has been implemented:

$$v(t; t_{\text{per}}, t_{\text{src}}, t_{\text{trs}}, \xi, \zeta) = \frac{1}{2} \sum_{n=0}^{\infty} \left[\operatorname{erf} \left(\xi \left(\zeta \frac{t - n t_{\text{per}}}{t_{\text{trs}}} - 1 \right) \right) - \operatorname{erf} \left(\xi \left(\zeta \frac{t - n t_{\text{per}} - t_{\text{src}}}{t_{\text{trs}}} - 1 \right) \right) \right]. \quad (4)$$

Here $\operatorname{erf}(t)$ is the error function [7, 8].

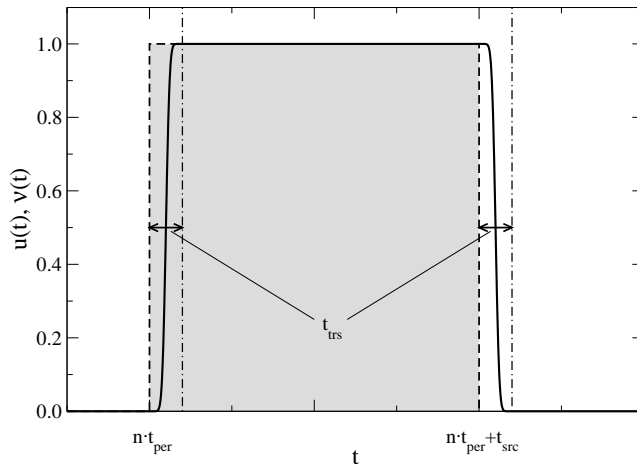


Figure 2. Dashed line: the periodic step function $u(t)$ as a combination of the Heaviside ones. Solid line: the “realistic” source function for $\xi = 4$ and $\zeta = 2$ representing the transient model. The dot-dashed lines show the ends of the transient process at “turn on” and “turn off”

Such smoothing of the processes of “turn on” and “turn off” of the source also helps to stabilize numerical simulations.

The initial condition can be set by the assumption that at $t = 0$ the cryogenic cell has been already cooled down by the temperature terminal:

$$T(r, z, t = 0) = T_0, \quad (5)$$

where $T_0 \equiv 4.2 \text{ K}$ is the temperature of liquid helium.

The boundary conditions can be expressed after the assumption that the temperature flow across the boundary of the domain is zero except for the right side where a connection to the temperature terminal exists (see Fig. 1):

$$\begin{cases} \frac{\partial T}{\partial \mathbf{n}} = 0 & \forall (r, z) \in \delta\Omega \setminus \{(r, z) : z = z_{\max}\}, \\ T = T_0 & \forall (r, z) \in \{(r, z) : z = z_{\max}\}, \end{cases} \quad (6)$$

where $\delta\Omega$ is the boundary of the domain Ω , \mathbf{n} is the normal vector of the boundary $\delta\Omega$. This assumption is motivated by the following statements:

- the cryonics cell is installed in the vacuum chamber, therefore, there is no convective heat transfer;
- the working temperature is too low for the appearance of thermal radiation;
- we neglect the energy for evaporation of gas molecules;
- there is no temperature flow through the axis $r = 0$ due to the axial symmetry.

3. Discretization and numerical method

Numerical solution of Eq. (1) can be obtained by using a shifted non-uniform grid (see Fig. 3):

$$\begin{aligned} \bar{\omega} = \{ & (t, r, z) \mid 0 \leq t < \infty, \quad t_{k+1} = t_k + \tau_{k+1}, \quad k \in \mathbb{N}_0; \\ & 0.5h_1 \leq r \leq r_{\max} - 0.5h_{N_j-1}, \quad r_{i+1} = r_i + h_{i+1}, \quad i = 0, \dots, N_j - 1; \\ & 0.5\eta_1 \leq z \leq z_{\max} - 0.5\eta_{M_i-1}, \quad z_{j+1} = z_j + \eta_{j+1}, \quad j = 0, \dots, M_i - 1\}. \end{aligned} \quad (7)$$

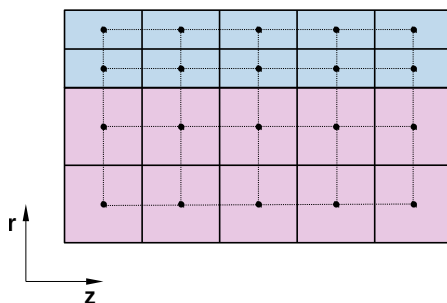


Figure 3. The discretization of the 2D domain. The non-uniform grid is shifted in order to have points at the centers of boxes. Different layers (materials) have different step size (they are differently colored)

It seems usual to make uniform steps in the subdomain corresponding one layer. The shifted grid has no points at the boundary of discontinuity. One can also use a special grid – the grid with points at the boundary of materials, in this case one has to take care of approximation of the thermal coefficients and the source function at the boundary.

The initial boundary value problem Eqs. (1)–(6) has been approximated on the grid (7) by the alternating direction implicit (ADI) schemes [9–12]:

$$\bar{\rho}_{i,j} \bar{c}_{V i,j} \frac{\bar{T}_{i,j} - T_{i,j}}{0.5\tau} = \Lambda_r [\bar{T}_{i,j}] + \Lambda_z [T_{i,j}] + \bar{X}_{i,j}, \quad (8)$$

$$\bar{\rho}_{i,j} \bar{c}_{V i,j} \frac{\hat{T}_{i,j} - \bar{T}_{i,j}}{0.5\tau} = \Lambda_r [\bar{T}_{i,j}] + \Lambda_z [\hat{T}_{i,j}] + \bar{X}_{i,j}, \quad (9)$$

where $\hat{T}_{i,j}$ is the temperature distribution on the next time layer, $\bar{T}_{i,j}$ is the temperature distribution on the half layer (in between the next and current time layers), $T_{i,j}$ is the value on the current time layer and τ is the time step,

$$\bar{\rho}_{i,j} = \rho(\bar{T}_{i,j}), \quad \bar{c}_{V i,j} = c_V(\bar{T}_{i,j}), \quad \bar{X}_{i,j} = X(\bar{T}_{i,j}).$$

The spatial finite difference operators in Eqs. (8) and (9) are:

$$\Lambda_r [T_{i,j}] = \frac{1}{r_i} \frac{1}{\bar{h}_i} \left[r_{i+\frac{1}{2}} \lambda_{i+\frac{1}{2},j} \frac{T_{i+1,j} - T_{i,j}}{h_{i+1}} - r_{i-\frac{1}{2}} \lambda_{i-\frac{1}{2},j} \frac{T_{i,j} - T_{i-1,j}}{h_i} \right], \quad (10)$$

$$\Lambda_z [T_{i,j}] = \frac{1}{\eta_j} \left[\lambda_{i,j+\frac{1}{2}} \frac{T_{i,j+1} - T_{i,j}}{\eta_{j+1}} - \lambda_{i,j-\frac{1}{2}} \frac{T_{i,j} - T_{i,j-1}}{\eta_j} \right], \quad (11)$$

where $i = 1, \dots, N_j - 1$, $j = 1, \dots, M_i - 1$, $h_i = r_i - r_{i-1}$, $\eta_j = z_j - z_{j-1}$, $\bar{h}_i = (h_{i+1} + h_i)/2$, $\eta_j = (\eta_{j+1} + \eta_j)/2$, $\lambda_{i,j} = \lambda_m(T_{i,j})$, $c_{V i,j} = c_{V m}(T_{i,j})$, $X_{i,j} = X_m(T_{i,j})$, $r_{i\pm 1/2} = (r_i + r_{i\pm 1})/2$, $\lambda_{i\pm 1/2,j} = \lambda_m(T_{i,j} + T_{i\pm 1,j})/2$, $\lambda_{i,j\pm 1/2} = \lambda_m(T_{i,j} + T_{i,j\pm 1})/2$.

Due to the non-linearity of Eqs. (8)–(9) (when the thermal coefficients and the source function depend on temperature) the simple-iteration method has been applied for calculation of the sought-for function on the half and next time layers. The recursive forms for (8)–(9) are expressed as follows [11–13]:

$$\begin{aligned} \rho_{i,j}^s c_{V i,j}^s \frac{T_{i,j}^{s+1} - T_{i,j}^s}{0.5\tau} = \\ = \frac{1}{r_i} \frac{1}{\bar{h}_i} \left[r_{i+\frac{1}{2}} \lambda_{i+\frac{1}{2},j}^s \frac{T_{i+1,j}^{s+1} - T_{i,j}^{s+1}}{h_{i+1}} - r_{i-\frac{1}{2}} \lambda_{i-\frac{1}{2},j}^s \frac{T_{i,j}^{s+1} - T_{i-1,j}^{s+1}}{h_i} \right] + \\ + \Lambda_z [T_{i,j}] + X_{i,j}^s, \quad (12) \end{aligned}$$

here it is assumed that when $s \rightarrow \infty$, then $T^s \rightarrow \bar{T}$, $\rho^s \rightarrow \bar{\rho}$, $c_V^s \rightarrow \bar{c}_V$, $\lambda^s \rightarrow \bar{\lambda}$, and $X^s \rightarrow \bar{X}$.

The iteration process starts with the initial condition that $T_{i,j}^{s=0} = T_{i,j}$, and stops after fulfilling the following criteria

$$\|T^{s+1} - T^s\|_C = \max_{\bar{\omega}} \|T^{s+1} - T^s\| < \varepsilon. \quad (13)$$

The values of the sought-for function on next time-layer are obtained as this

$$\begin{aligned} & \frac{\bar{\rho}_{i,j} \bar{c}_{V,i,j}}{0.5\tau} \frac{T_{i,j}^{s+1} - \bar{T}_{i,j}}{0.5\tau} = \\ & = \Lambda_r [\bar{T}_{i,j}] + \frac{1}{\eta_j} \left[\lambda_{i,j+\frac{1}{2}}^s \frac{T_{i,j+1}^{s+1} - T_{i,j}^{s+1}}{\eta_{j+1}} - \lambda_{i,j-\frac{1}{2}}^s \frac{T_{i,j}^{s+1} - T_{i,j-1}^{s+1}}{\eta_j} \right] + \bar{X}_{i,j}, \quad (14) \end{aligned}$$

with the initial condition $T_{i,j}^{s=0} = \bar{T}_{i,j}$. Same as before $T^{s \rightarrow \infty} \rightarrow \hat{T}$ and $\lambda^{s \rightarrow \infty} \rightarrow \hat{\lambda}$. This iteration process stops after fulfilling the same criteria (13). The systems of linear algebraic equations (12) and (14) are solved by the Thomas method [13–15].

In order to ensure convergence of the iteration process (12)–(14), the adaptive time-step has been implemented. If the counter of iterations s exceeds some maximal value, meaning that the process does not converge fast enough, the time-step τ is divided by 2 and the iteration process is restarted (back to the Eq. (12)).

4. Parallel algorithm

Main computational complexity comes from repetitive calculation of Eqs. (12) and (14) across each time layer. A solution of the first of them is needed as a start for solving the second one and it is again used as a start for calculation of the sought-for function on the next time layer. Due to rather low complexity of solving of one system of linear equations ((12) or (14)) it is better to use parallelization based on shared memory since for distributed memory parallelization the cost of data transfer would be too high. Therefore, we opted for OpenMP [16, 17].

In Fig. 4 one can see the flowchart of the algorithm. After initializing the solution – setting t_{prd} , t_{src} , I , and $t_0 = 0$, the program repeats iterations until the requested time is reached. In one step of evolution it first initializes the estimate of the time step τ as being equal $t_{\text{trs}}/1000$ if we are in the transition process or $t_{\text{src}}/100$ elsewhere. After this it starts the iteration process in order to obtain the solution $\bar{T}_{i,j}$ at the time $t_k + \tau/2$ using (12). If the obtained solution is precise enough, it alternates direction and continues by the way of (14) to the solution $\hat{T}_{i,j}$ at the time $t_k + \tau$. If this solution is again precise enough, the algorithm sets the total time to $t_k = t_{k-1} + \tau$ and the actual solution $T_{i,j} = \hat{T}_{i,j}$. If in any of the previous tests the number of iterations exceeds the number of maximum iterations (iter – see Fig. 4), then the time-step τ is divided by 2 and the calculation returns to the beginning of the evolution step.

The whole algorithm terminates when the total time t reaches the desired value or when we realize that we have entered into the periodic process (temperature changes periodically depending on switching the current in conductive layer on and off).

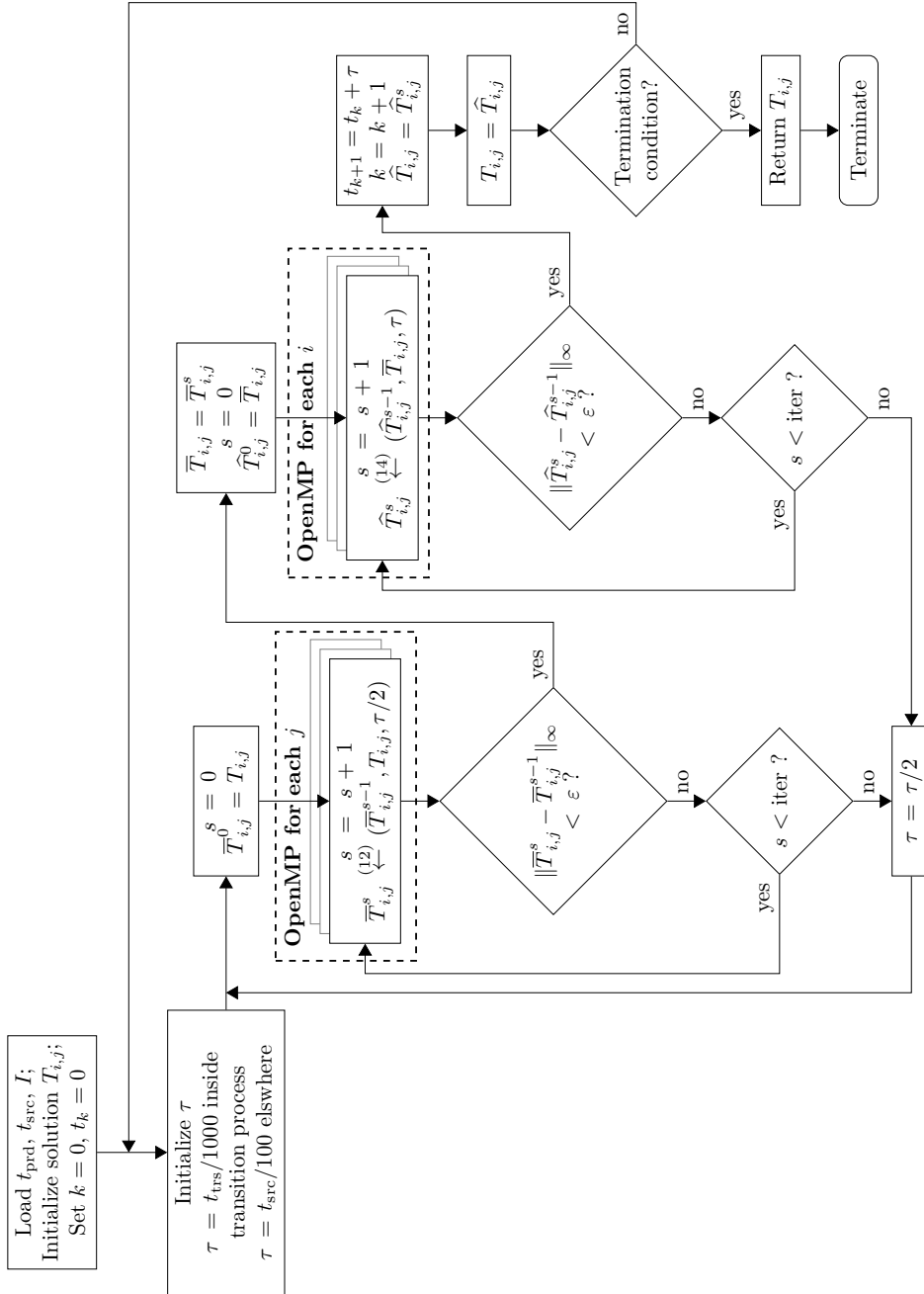


Figure 4. Schematics of the algorithm with parts running using OpenMP highlighted by the dashed line

5. Numerical results

The calculations have been performed on the HybriLIT computational platform [18, 19] using the Skylake processor Intel Xeon Gold 6154 [20] containing 18 CPU cores providing two threads per core (36 threads in total) under OS Scientific Linux 7.5 (Nitrogen) [21].

As an example we have studied the case when $t_{\text{per}} = 10^{-1}$, $t_{\text{src}} = 10^{-2}$, $t_{\text{trs}} = 10^{-4}$, and $I_0 = 0.5742$. These values of parameters were chosen to realize the “thermal gates” for maximal and minimal critical temperatures 42 K and 37 K, respectively [22]. The cell size was selected as follows: $z_0 = 4$, $z_{\text{max}} = 5$, $r_0^* = 0.24$, $r_1^* = 0.245$, $r_2^* = 0.25$, $r_{\text{max}} = 0.2501$. The whole domain was split into 100 parts along the z axis at the first layer (core) and to 80 in the other layers. Along the r axis, individual layers were divided (starting from the core) into 800, 200, 200, and 10 parts respectively. This discretization of the domain was chosen in order not to split the domain into too many parts and at the same time have enough information about the solution. It is noteworthy that we have much more steps in the radial direction. It is so because we expect the flow in-between the layers to be more active than the relaxation towards the terminal. Nevertheless, in our experiments we have also densified the grid to see the impact of the grid on both the precision of the solution and the calculation time. The results are given in Fig. 5, it shows the temperature fields at different moments of evolution inside the required steady periodic temperature regime.

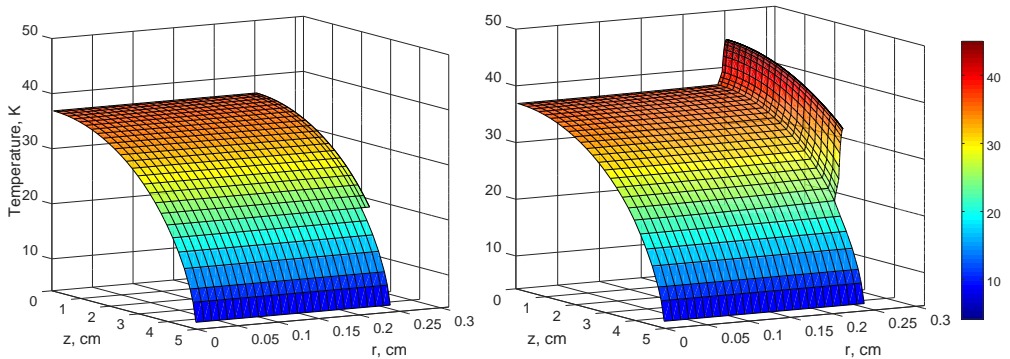


Figure 5. Temperature fields when the periodic temperature regime is achieved. *Left* panel: the temperature field at the moment before turning on the source. *Right* panel: the temperature field at the moment when the source was just turned off

The field is shown in the whole cylindrical domain right before turning on the source (at the left panel). The field is in a state of maximum relaxation in that moment. At the right side the temperature field is shown in the moment when source is turning off. The results demonstrate that temperature significantly changes only in outer layers, the core rode is practically not heated, it works as thermostat. The evolution of the temperature at the surface of the cryogenic cell at the $z = 0$ is given in Fig. 6, it is evident that it takes time to achieve the required steady periodic temperature regime.

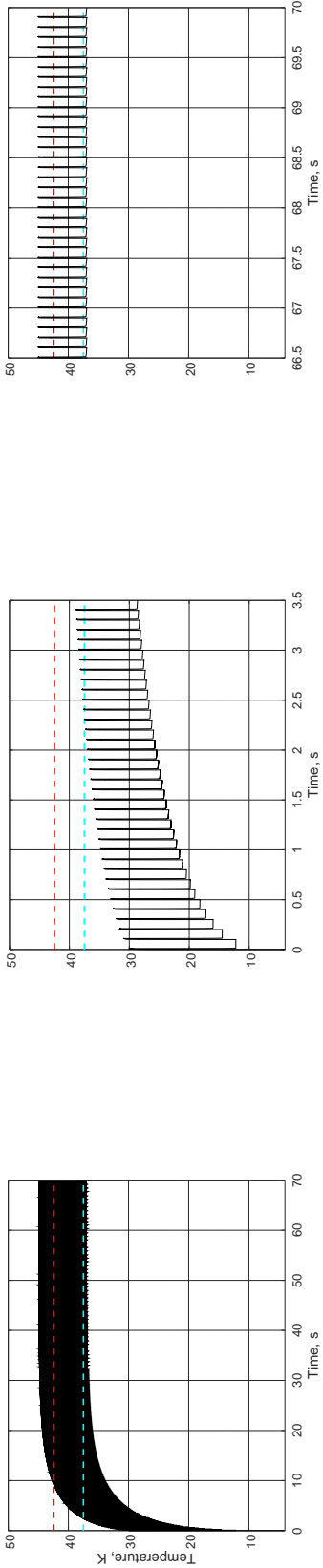


Figure 6. Temperature evolution on the surface at the $z = 0$ (black line). Red colored upper dashed line represents the maximal critical temperature (42 K) and blue colored lower dashed line represents the minimal critical temperature (37 K). *Left panel:* Temperature dependence on the time from 0 up to 70 sec. *Central panel:* the beginning of the evolution (the first 3.5 sec.). *Right panel:* the last 3.5 sec. of the evolution when the periodic steady temperature regime is achieved

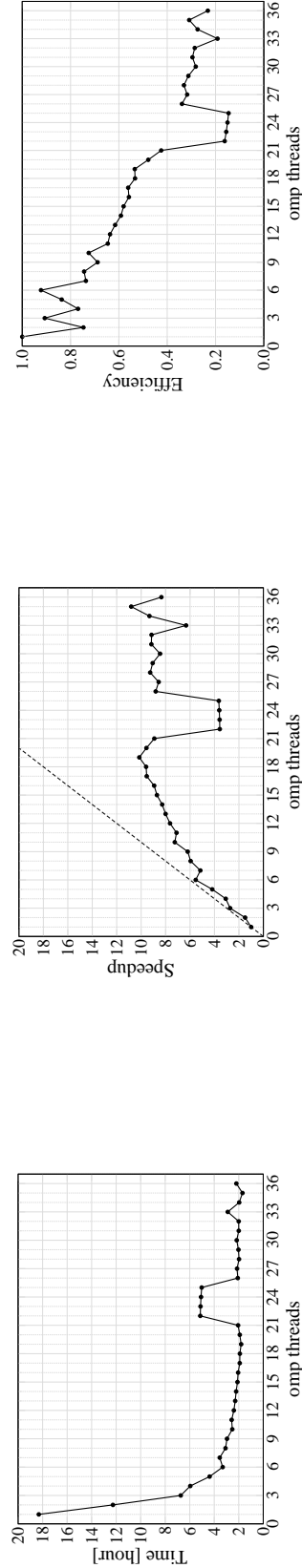


Figure 7. The experimental performance of the algorithm. *Left panel:* the calculation time in hours. *Central panel:* the speed up of calculations. *Right panel:* the efficiency of parallelization

6. Summary and conclusions

We have developed the algorithm for numerical simulations of heat evolution inside the multilayered cylindrical domain with the periodic source. One can see from Fig. 6 that the required periodical temperature regime cannot be obtained immediately, it has a setup mode which is much longer than one period, thus it has to be taken into account when designing the pulse cryogenic cell. The simulations show the possibility of the realization of “thermal gates” for a particular set of parameters. The algorithm has been integrated to the hybrid algorithm MPI+OpenMP for solving the optimization problem of the heat source characteristics (t_{per} , t_{src} , and I_0) of the pulse cryogenic cell [22].

The performance of the parallel algorithm (see Fig. 7) is in agreement with the case studies in literature, e.g., [23, 24]. As it is shown in the picture that the saturation calculation time been achieved at 18 threads, after acting the hyper-threading the speedup stops. Thus there is no reason to involve in calculations more than this number of threads for the considered problem with the given grid size (1210×100).

Acknowledgments

Authors thank H. Grigorian, E. E. Donets and E. Ayryan for fruitful discussions and help, it has allowed to improve the article. The work has been partially supported by the Russian Foundation for Basic Research under the projects № 18-51-18005 and № 19-01-00645. Computations have been conducted on the basis of the HybriLIT heterogeneous computing platform (LIT, JINR).

References

1. D. E. Donets, E. E. Donets, T. Honma, K. Noda, A. Y. Ramzdorf, V. V. Salmikov, V. B. Shutov, E. D. Donets, Physics research and technology developments of electron string ion sources, *Review of Scientific Instruments* 83 (2012) 02A512. doi:10.1063/1.3678660.
2. K. Katagiri, A. Noda, K. Suzuki, K. Nagatsu, A. Y. Boytsov, D. E. Donets, E. D. Donets, E. E. Donets, A. Y. Ramzdorf, M. Nakao, S. Hojo, T. Wakui, K. Noda, Cryogenic molecular separation system for radioactive ^{11}C ion acceleration, *Review of Scientific Instruments* 86 (12) (2015) 123303. doi:10.1063/1.4937593.
3. A. Ayriyan, J. Buša Jr., E. E. Donets, H. Grigorian, J. Pribiš, Algorithm and simulation of heat conduction process for design of a thin multi-layer technical device, *Applied Thermal Engineering* 94 (2016) 151–158. doi:10.1016/j.applthermaleng.2015.10.095.
4. R. E. Honig, H. O. Hook, Vapor pressure data for some common gases, David Sarnoff Research Center, RCA, Princeton, 1960.
5. D. B. Chelton, D. B. Mann, *Cryogenic data book* (1956).
6. P. Symons, *Digital waveform generation*, Cambridge University Press, New York, 2013.
7. M. Abramowitz, I. A. Stegun, *Handbook of mathematical functions*, Tenth Edition, Dover Publications, New York, 1972.

8. G. A. Korn, T. M. Korn, *Mathematical handbook for scientists and engineers*, Revised Edition, Dover Publications, New York, 2013.
9. D. W. Peaceman, H. H. Rachford Jr., The numerical solution of parabolic and elliptic differential equations, *Journal of the Society for Industrial and Applied Mathematics* 3 (1955) 28–41.
10. N. N. Yanenko, *Fractional step methods for solution of multidimensional problems of mathematical physics [Metod drobnykh shagov resheniya mnogomernykh zadach]*, Nauka, Moscow, 1967, in Russian.
11. A. A. Samarskii, P. N. Vabishchevich (Eds.), *Additive difference schemes for problems of mathematical physics [Additivnyye skhemy dlya zadach matematicheskoy fiziki]*, Nauka, Moscow, 1999, in Russian.
12. A. A. Samarsky, *The theory of difference schemes*, Marcel Dekker Inc., New York, 2001.
13. N. N. Kalitkin, *Numerical methods [Chislennyye metody]*, Second Edition, BHV-Peterburg, Saint Petersburg, 2013, in Russian.
14. L. H. Thomas, *Elliptic problems in linear differential equations over a network*, Tech. rep., Columbia University, New York (1949).
15. A. A. Samarskii, P. N. Vabishchevich, *Computational heat transfer*, Vol. 1, John Wiley & Sons Ltd., Chichester, England, 1995.
16. L. Dagum, R. Menon, OpenMP: an industry standard API for shared-memory programming, *Computational Science & Engineering*, IEEE 5 (1) (1998) 46–55.
17. OpenMP Architecture Review Board, *OpenMP application programming interface version 5.0* (November 2018).
URL <https://www.openmp.org/wp-content/uploads/OpenMP-API-Specification-5.0.pdf>
18. HybriLIT group, *Heterogeneous platform “HybriLIT”* [cited 14.01.2019].
URL <http://hlit.jinr.ru/en/>
19. G. Adam, M. Bashashin, D. Belyakov, M. Kirakosyan, M. Matveev, D. Podgainy, T. Sapozhnikova, O. Streltsova, S. Torosyan, M. Vala, L. Valova, A. Vorontsov, T. Zaikina, E. Zemlyanaya, M. Zuev, *IT-ecosystem of the HybriLIT heterogeneous platform for high-performance computing and training of IT-specialists*, in: V. Korenkov, A. Nechaevskiy, T. Zaikina, E. Mazhitova (Eds.), *CEUR Workshop Proceedings*, Vol. 2267, 2018, pp. 638–644.
20. Intel corporation, *Intel Xeon Gold 6154 Processor* [cited 14.01.2019].
URL <https://www.intel.com/content/www/us/en/products/processors/xeon/scalable/gold-processors/gold-6154.html>
21. Fermilab, CERN, *Scientific Linux* [cited 14.01.2019].
URL <http://scientificlinux.org>
22. A. Ayriyan, J. B. Jr., H. Grigorian, E. E. Donets, *Solving the optimization problem for designing a pulsed cryogenic cell*, *Physics of Particles and Nuclei Letters* 16 (5) (2019 (Accepted to print)) 300–309. doi:10.1134/S1547477119030026.
23. V. A. Tokareva, O. I. Streltsova, M. I. Zuev, *Parallel realizations of locally one-dimensional difference schemes for solving the initial-boundary value problems for the multidimensional heat equation*, in: A. V. Friesen, V. Chudoba (Eds.), *Proceedings of the XX International Scientific Conference of Young Scientists and Specialists (AYSS-2016)*, 2016, pp. 142–147.

24. M. D. Schuster, The heat equation: high-performance scientific computing case study, *Computing in Science & Engineering* 20 (5) (2018) 114–127. doi:10.1109/MCSE.2018.05329820.

For citation:

A. Ayriyan, J. Buša Jr., Parallel algorithm for numerical solution of heat equation in complex cylindrical domain, *Discrete and Continuous Models and Applied Computational Science* 27 (1) (2019) 21–32. DOI: 10.22363/2658-4670-2019-27-1-21-32.

Information about the authors:

Alexander S. Ayriyan (Russian Federation) — researcher of the Laboratory of Information Technologies, Joint Institute for Nuclear Research (e-mail: ayriyan@jinr.ru, phone: +7(496)216-35-98, ORCID: <https://orcid.org/0000-0002-5464-4392>, ResearcherID: O-5259-2015, Scopus Author ID: 24528624400)

Ján Buša Jr. (Russian Federation) — PhD in Mathematics, Senior Researcher of the Laboratory of Information Technologies, Joint Institute for Nuclear Research (e-mail: busa@jinr.ru, phone: +7(496)216-35-98, ORCID: <https://orcid.org/0000-0003-3807-0373>, ResearcherID: AAB-6463-2019, Scopus Author ID: 57188571341)



UDC 512, 519.6

DOI: 10.22363/2658-4670-2019-27-1-33-41

The symbolic problems associated with Runge–Kutta methods and their solving in Sage

Yu Ying^{1,2}

¹ Department of Applied Probability and Informatics
Peoples' Friendship University of Russia (RUDN University)
6, Miklukho-Maklaya str., Moscow, 117198, Russian Federation

² Department of Algebra and Geometry
Kaili University
3, Kaiyuan Road, Kaili, 556011, China

(received: February 21, 2019; accepted: October 21, 2019)

Runge–Kutta schemes play a very important role in solving ordinary differential equations numerically. At first we want to present the Sage routine for calculation of Butcher matrix, we call it an rk package. We tested our Sage routine in several numerical experiments with standard and symplectic schemes and verified our result by corporation with results of the calculations made by hand.

Second, in Sage there are the excellent tools for investigation of algebraic sets, based on Gröbner basis technique. As we all known, the choice of parameters in Runge–Kutta scheme is free. By the help of these tools we study the algebraic properties of the manifolds in affine space, coordinates of whose are Butcher coefficients in Runge–Kutta scheme. Results are given both for explicit Runge–Kutta scheme and implicit Runge–Kutta scheme by using our rk package. Examples are carried out to justify our results. All calculation are executed in the computer algebra system Sage.

Key words and phrases: Symplectic Runge–Kutta Scheme; Gröbner basis, Sage, Sagemath

1. Introduction

The Runge–Kutta method is the most popular numerical method for solving of ordinary differential equations (ODE), however the development of this method indicates some symbolic problems.

Let's review some results on Runge–Kutta scheme [1]. For an autonomous system

$$\dot{\vec{x}} = \vec{F}(\vec{x}) \quad (1)$$

Runge–Kutta scheme with s stages can be written as

$$\vec{k}_i = \vec{F} \left(\vec{x} + dt \sum_{j=1}^s a_{ij} \vec{k}_j \right), \quad i = 1, 2, \dots, s \quad (2)$$



and

$$\hat{\vec{x}} = \vec{x} + dt \sum_{i=1}^s b_i \vec{k}_i. \quad (3)$$

We will write the coefficients a_{ij} and b_i in Butcher matrix, for example, for $s = 2$

$$\begin{array}{c|cc} c_1 & a_{11} & a_{12} \\ c_2 & a_{21} & a_{22} \\ \hline & b_1 & b_2 \end{array}$$

Hereinafter $c_i = \sum_{j=1}^s a_{ij}$.

These coefficients are selected in such a way that the difference scheme approximates the ODE (1) with some order p . For $s = p = 4$ appropriate numerical values for the coefficients was found by Kutta in the XIX century. The usage of Runge–Kutta scheme for the solving of given ODEs means the numerical calculations in the floating-point arithmetic.

However the problem about finding the coefficients of Butcher matrix is pure algebraic, so now we can try to solve it with the help of computer algebra systems like Sage or Maple [2–4]. This is the first symbolic problem associated with Runge–Kutta method. In our paper we want to present our algorithms for symbolical calculation of the Butcher matrix and its realization in Sage.

It should be noted that conditions of approximation and other conditions don't define the coefficients of Butcher matrix unambiguously. From geometrical point of view the list of coefficients of Butcher matrix is a point in affine space (Butcher space) and appropriate points form a variety in this space. As in Sage there are some tools for a research of a set of solutions of systems of the algebraic equations, we can try to describe the varieties in Butcher spaces.

The Runge–Kutta scheme is explicit iff $a_{ij} = 0$, $j \geq i$, in this case the numerical calculation doesn't demand the solving of nonlinear algebraic equations. This is the most investigated case, for small s the Butcher varieties were described by Butcher himself, now we know approximate values of a_{ij} for schemes with $s = 9$ [5–7].

The implicit Runge–Kutta scheme is interesting because they can save some symbolic properties of exact solution. By Cooper theorem symplectic Runge–Kutta scheme saves exactly all quadratic integrals of motion [8, 9]. The symplecticity gives algebraic conditions for Butcher matrix, and we can try to investigate the varieties in Butcher space by the help of Sage.

In our numerical experiments these varieties were rational with singularity at point with $a_{ij} = 0$ at all values of i and j . Thus there are infinite set of Butcher matrices with rational coefficients.

Organization of calculations by the implicit Runge–Kutta scheme demands solving of algebraic equations at each step. Investigation of the algebraic system is the second symbolic problem associated with Runge–Kutta scheme which we can try to solve by Sage.

2. The problem of finding coefficients of Butcher matrix, approximative conditions

In this part, we try to set up a program for finding Runge–Kutta scheme when s is number of the stages and p is order of approximation. This scheme we can call $\mathbf{rk}(s, p)$. Butcher matrix is square matrix of degree s . Condition of approximation is algebraic equation with respect of elements of Butcher matrix. Firstly, we note that these equations don't depend on the number of the approximative differential equations, so we can only consider the first order equation $\dot{x} = f(x)$.

The Taylor series for the solution satisfying the zero initial condition $x(t_0) = 0$ are

$$x(t) = D(f)|_{x=0} (t - t_0) + D^2(f)|_{x=0} \frac{(t - t_0)^2}{2!} + \dots,$$

where

$$D = f \frac{d}{dx}.$$

At $t = t_1$ we have

$$x(t_1) = D(f)|_{x=0} dt + D^2(f)|_{x=0} \frac{dt^2}{2!} + \dots, \quad (4)$$

where $dt = t_1 - t_0$.

The first step of Runge–Kutta scheme with s stages can be written as

$$k_i = f \left(dt \sum_{j=1}^s a_{ij} k_j \right), \quad i = 1, 2, \dots, s \quad (5)$$

and

$$\hat{x} = dt \sum_{i=1}^s b_i k_i. \quad (6)$$

Let the power series for the solution of systems (5) be

$$k_i = k_{i,0} + k_{i,1} dt + k_{i,2} dt^2 + \dots$$

Manually or in computer algebra system we can find their coefficients by recursion. So at $dt = 0$ the equations (5) give us

$$k_{i,0} = f(0).$$

To find the coefficients at dt , we differentiate the equations (5) with respect to dt and substitute $dt = 0$, then we have

$$k_{i,1} = f'(0) \cdot \left(\sum_{j=1}^s a_{ij} k_{j,0} \right), \quad i = 1, 2, \dots, s.$$

To find the coefficients of dt^2 , we differentiate the equations (5) twice and substitute $dt = 0$ again, etc. Substituting the power series for k_i in (6) we have the power series for \hat{x} . By definition, the difference scheme has the p -th order approximation, if first p terms of the power series (4) for exact solution at $t = t_1$ and the power series for \hat{x} coincide. So, these are the required conditions of approximation written as a system of algebraic equations with respect to Butcher coefficients.

In the area of symbolic calculation, we consider the Butcher coefficients a, b as symbolical variables. We also consider the function f as arbitrary function of x , thus we may manipulate with its derivatives

$$f_0 = f(0), \quad f_1 = f'(0), \quad f_2 = f''(0), \dots$$

as independent symbolic variables. Comparing the coefficients at dt, \dots, dt^p in the way stated above, we get p algebraic equations, left sides of which belong to the polynomial ring

$$\mathbb{Q}[a, b][f_0, \dots, f_p].$$

By the arbitrariness of f , coefficients of all the monomials $f_0^{m_0} \dots$ must be zero. This gives us a number of equations for the coefficients of Butcher matrix, which are the required equations. Thus the approximation conditions are algebraic equations, left sides of which belong to the ring $\mathbb{Q}[a, b]$ and form an ideal in $\mathbb{Q}[a, b]$. For brevity we will say that the approximation conditions generate the ideal.

In our package `rk.sage` function `rk_var(s)` gives all the necessary symbolical variables for the coefficients a, b and ring

$$K_{ab} = \mathbb{Q}[a_{11}, \dots, b_1, \dots]$$

for the scheme with s stages. As we know the condition of approximation with order p is the system of equations, the function `rk_series(s,p)` returns the left side of these equations. Let's review an example.

```
sage: var('x, t, dt')
(x, t, dt)
sage: load("rk.sage")
None
sage: rk_var(3)
None
sage: a
[a00 a01 a02]
[a10 a11 a12]
[a20 a21 a22]
sage: b
(b0, b1, b2)
sage: c
[a00 + a01 + a02, a10 + a11 + a12, a20 + a21 + a22]
```

So we have all Butcher coefficients. The construction

```
sage: rk_series(3,3)
```

return the result which coincides with the statement in the book of E. Hairer et al. [1, §II 2, theorem 2.1].

Any partial solution \bar{a}, \bar{b} of this algebraic equation system gives scheme type $\text{rk}(3,3)$. Also in our package it is possible to work only with explicit schemes.

```
sage: rk_var(3,implicit=false)
None
sage: a
[ 0  0  0]
[a10 0  0]
[a20 a21 0]
sage: b
(b0, b1, b2)
sage: c
[0, a10, a20 + a21]
sage: rk_series(3,3,implicit=false)
[-b0 - b1 - b2 + 1,
-2*a10*b1 - 2*a20*b2 - 2*a21*b2 + 1,
-6*a10*a21*b2 + 1,
-3*a10^2*b1 - 3*a20^2*b2 - 6*a20*a21*b2 - 3*a21^2*b2 + 1]
```

This means that the affine variety of 3-stage Runge–Kutta scheme, approximating the differential equation with order 3, has 6 Butcher coefficients satisfying the 4 equations. These equations give some algebraic sets in the affine 6d-space. To study this set under Sage, we consider the corresponding ideal:

```
sage: J=Kab*rk_series(3,3,implicit=false)
sage: J.dimension()
2
sage: J.is_prime()
True
```

Thus, the set of coefficients formulate an irreducible surface. Its projection in the 3-dimension space a_{10}, a_{20}, a_{21} is a cubic surface:

```
sage: J.elimination_ideal([Kab(b0),Kab(b1),Kab(b2)])
Ideal
(3*a10^2*a21 - a10*a20 - 3*a10*a21 + a20^2 + 2*a20*a21 + a21^2)
of Multivariate Polynomial Ring in a10, a20, a21, b0, b1, b2
↪ over Rational Field
```

Since the linear family of right lines passing through the point O intersects this surface at one moving point, so this surface is rational.

We try investigate $\text{rk}(4,4)$ in Sage. Our program give system of equations very quickly but Sage can't calculate Gröbner basis of the ideal, generated by this system. We try use CAS Maple (which have several commercial routines for calculation Gröbner basis) but without success. It should be noted that this system was investigated by hand in the XIX century!

By using Sage we calculate the dimensions of the algebraic sets for explicit and implicit RK-schemes. Results are presented in the Tables 1 and 2. The analysis of RK-schemes with bigger p cannot be made in such a way that the Gröbner basis can be calculated.

Table 1

Dimensions for implicit Runge–Kutta scheme in the case of $1 < s < 4$; $1 < p < 4$

s, p	$p = 2$	$p = 3$
$s = 2$	4	2
$s = 3$	10	8

Table 2

Dimensions for explicit Runge–Kutta scheme on the case of $1 < s < 4$; $1 < p < 4$. The value -1 means that the set of Runge–Kutta scheme with given s and p is empty

s, p	$p = 2$	$p = 3$
$s = 2$	4	-1
$s = 3$	4	2

3. Symplectic Runge–Kutta schemes

We describe the manifold in the affine space ab , coordinates of whose points can be used as coefficients in the Runge–Kutta scheme, satisfying both the symplecticity and p -order approximation [8–10]. We denote this manifold as $S(s, p)$. We can find their equations in Sage like:

```
sage: rk_var(2)
None
sage: rk_symplectic(3,2)
[2*a00*b0 - b0^2,
a01*b0 + a10*b1 - b0*b1,
a01*b0 + a10*b1 - b0*b1, 2*a11*b1 - b1^2,
-b0 - b1 + 1,
-2*a00*b0 - 2*a01*b0 - 2*a10*b1 - 2*a11*b1 + 1,
-6*a00^2*b0 - 6*a00*a01*b0 - 6*a00*a10*b1 - 6*a01*a10*b0
  - 6*a01*a10*b1 - 6*a01*a11*b0 - 6*a10*a11*b1 - 6*a11^2*b1
  ↪ + 1,
-3*a00^2*b0 - 6*a00*a01*b0 - 3*a01^2*b0 - 3*a10^2*b1
  - 6*a10*a11*b1 - 3*a11^2*b1 + 1]
```

The tool of Sage allows you to describe this manifold. For example, for $S(2, 3)$ we have

```
sage: eqs = rk_symplectic(3,2)
sage: J=Kab*eqs
sage: J.dimension()
1
sage: J.is_prime()
True
```

So $S(2, 3)$ is irreducible curve. We can find its projection on any of the coordinate planes. In the $a_{00}a_{10}$ -plane its equation is

```
sage: J.elimination_ideal([Kab(b1),Kab(b0),Kab(a01),Kab(a11)])
Ideal
(12*a00^3 - 24*a00^2*a10 - 6*a00^2 + 12*a00*a10^2 + 12*a00*a10
↪ + a00 - 6*a10^2)
of Multivariate Polynomial Ring in a00, a01, a10, a11, b0, b1
↪ over Rational Field
```

We can calculate the genus of the curve of the 3rd order:

```
sage: elvars=[Kab(b1),Kab(b0),Kab(a00),Kab(a01)]
sage: F=J.elimination_ideal(elvars).gens()[0]
sage: KK=QQ[a10,a11]
sage: Curve(KK(F)).genus()
0
```

If genus of the curve is equal to zero the curve is rational and in Sage we can find the rational parametrization for given curve with the help of the construction

```
sage: Curve(KK(F)).rational_parameterization()
```

By using the elimination ideal technique we makes it easy to find that b_0, b_1, a_{00}, a_{01} are linearly of a_{10} and a_{11} , thus coefficients of Butcher matrix for $S(2, 3)$ can be expressed as rational functions of one parameter t :

$$\begin{array}{c|cc}
 c_1 & \frac{3t^2 - 12t + 12}{8t^2 - 24t + 24} & \frac{3t^3 - 8t^2 + 24t - 24}{8t^3 - 24t^2 + 24t} + \frac{t^3 - 8t^2 - 24t - 24}{6t(t - 2)^2} \\
 c_1 & \frac{-t^3 + 8t^2 - 24t + 24}{8t^3 - 24t^2 + 24t} & \frac{t^2}{8t^2 - 24t + 24} \\
 \hline
 & 1 - \frac{1}{4} \frac{t^2}{t^2 - 3t + 3} & \frac{t^2}{4t^2 - 12t + 12}
 \end{array}$$

For example at the value $t = 3 \pm \sqrt{3}$ we have the scheme used by Nuan et al. [11, f. (24)]. At rational curve there are the infinite set of rational points thus there are infinite set of Runge–Kutta schemes of type $S(2, 3)$ with rational coefficients. For example at $t = 1$ we have

$$\begin{array}{c|cc}
 1/3 & 3/8 & -1/24 \\
 1 & 7/8 & 1/8 \\
 \hline
 & 3/4 & 1/4
 \end{array}$$

Increase in number of stages is interfered by difficulties, associated with the algorithm of calculation of Gröbner basis. We try investigating the case $s = 4$ in Maple, where there are several non-free algorithms of calculation of Gröbner basis, but without success.

In our numerical experiments the variate $S(s, p)$ with maximal value of p at fixed value of s has the dimension 1 and the genus 0 and thus is a rational curve in Butcher space. In practice it is important that there is an infinite number of sets of rational values for Butcher coefficients.

4. Conclusion

In this article we investigated one of the symbolic problems associated with Runge–Kutta method, namely the problem of calculation of Butcher matrix. We tested our Sage routine in several numerical experiments and verified our results by comparing them with the results of calculations made by hand.

We saw that computer algebra systems was ready to solve this problem and gave us some tools for investigation of the set of Butcher matrices. These tools indicate in our numerical experiments that Butcher coefficients were rational functions of one or two parameters and thus there is an infinite number of sets of rational values for Butcher coefficients. Perhaps, this property can be proved for Runge–Kutta schemes with any number of stages. This question requires further study. Also we can't calculate Gröbner basis of the ideals generated at $s > 3$. Perhaps, a successful substitution can solve this issue.

Acknowledgments

The publication has been prepared with the support of the “RUDN University Program 5-100” and funded by RFBR according to the research projects No. 18-07-00567 and No. 18-51-18005.

References

1. E. Hairer, G. Wanner, S. P. Nørsett, Solving ordinary differential equations, 3rd Edition, Vol. 1, Springer, New York, 2008.
2. The Sage Developers, SageMath, the Sage Mathematics Software System (Version 7.4) (2016).
URL <https://www.sagemath.org>
3. W. Stein, D. Joyner, SAGE: system for algebra and geometry experimentation, ACM SIGSAM Bulletin 39 (2) (2005) 61–64.
4. A. Y. Golubkov, A. I. Zobnin, S. O. V., Computer algebra in the Sage system. Manual [Komp'yuternaya algebra v sisteme Sage. Uchebnoye posobiye], Bauman Moscow State Technical University, Moscow, 2013, in Russian.
5. S. I. Khashin, A symbolic-numeric approach to the solution of the Butcher equations, Canadian Applied Mathematics Quarterly 17 (3) (2009) 555–569.
6. S. I. Khashin, Butcher algebras for Butcher systems, Numerical Algorithms 63 (4) (2013) 679–689. doi:10.1007/s11075-012-9647-x.
7. J. H. Verner, Explicit Runge–Kutta pairs with lower stage-order, Numerical Algorithms 65 (3) (2014) 555–577. doi:10.1007/s11075-012-9647-x.
8. E. Hairer, G. Wanner, C. Lubich, Geometric numerical integration. Structure-preserving algorithms for ordinary differential equations, 2nd Edition, Springer, New York, 2000.
9. J. M. Sanz-Serna, Symplectic Runge–Kutta schemes for adjoint equations, automatic differentiation, optimal control, and more, SIAM REVIEW 58 (1) (2016) 3–33. doi:10.1137/151002769.

10. M. N. Gevorkyan, J. V. Gladysheva, Symplectic integrators and the problem of wave propagation in layered media, *Bulletin of Peoples' Friendship University of Russia. Series: Mathematics. Information Sciences. Physics* (1) (2012) 50–60, in Russian.
11. Nuan Fang Xu, Zi-Chen Deng, Yan Wang, Kai Zhang, A symplectic Runge-Kutta method for the analysis of the tethered satellite system, *Multidiscipline Modeling in Materials and Structures* 13 (1) (2017) 26–35. doi:10.1108/MMMS-11-2016-0060.

For citation:

Yu. Ying, The symbolic problems associated with Runge–Kutta methods and their solving in Sage, *Discrete and Continuous Models and Applied Computational Science* 27 (1) (2019) 33–41. DOI: 10.22363/2658-4670-2019-27-1-33-41.

Information about the authors:

Yu Ying (China) — postgraduate student of Department of Applied Probability and Informatics of Peoples' Friendship University of Russia (RUDN University); assistant professor of Department of Algebra and Geometry, Kaili University (e-mail: yingy6165@gmail.com, phone: +7(495)9550927, ORCID: <https://orcid.org/0000-0002-4105-2566>, ResearcherID: AAC-8344-2019, Scopus Author ID: 57208127921)



UDC 512, 519.6

DOI: 10.22363/2658-4670-2019-27-1-42-48

Software for the numerical solution of first-order partial differential equations

Yaroslav Yu. Kuziv

*Department of Applied Probability and Informatics
Peoples' Friendship University of Russia (RUDN University)
6, Miklukho-Maklaya str., Moscow, 117198, Russian Federation*

(received: June 29, 2019; accepted: October 21, 2019)

Partial differential equations of the first order, arising in applied problems of optics and optoelectronics, often contain coefficients that are not defined by a single analytical expression in the entire considered domain. For example, the eikonal equation contains the refractive index, which is described by various expressions depending on the optical properties of the media that fill the domain under consideration. This type of equations cannot be analysed by standard tools built into modern computer algebra systems, including Maple.

The paper deals with the adaptation of the classical Cauchy method of integrating partial differential equations of the first order to the case when the coefficients of the equation are given by various analytical expressions in the subdomains G_1, \dots, G_k , into which the considered domain is divided. In this case, it is assumed that these subdomains are specified by inequalities. This integration method is implemented as a Python program using the SymPy library. The characteristics are calculated numerically using the Runge–Kutta method, but taking into account the change in the expressions for the coefficients of the equation when passing from one subdomain to another. The main functions of the program are described, including those that can be used to illustrate the Cauchy method. The verification was carried out by comparison with the results obtained in the Maple computer algebra system.

Key words and phrases: eikonal, partial differential equation, SymPy

Introduction

Partial differential equations (PDE) of the first order arise in many applied problems. The specificity of the problems in optics and optoelectronics is that the coefficients of these equations are not defined by a single analytical expression in the entire considered domain. Thus, for example, the eikonal equation is a nonlinear first-order PDE, one of whose coefficients is the refractive index, which is described by various expressions depending on the optical properties of the media filling the considered domain [1]. The same applies to the differential equations used to calculate the wave fronts and

© Kuziv Ya. Yu., 2019



This work is licensed under a Creative Commons Attribution 4.0 International License

<http://creativecommons.org/licenses/by/4.0/>

amplitudes in wave optics [2] or in the framework of the adiabatic waveguide method (AWM) proposed by A. A. Egorov and L. A. Sevastyanov [3–5].

The standard method for integrating nonlinear PDE is the characteristic method [6, 7], proposed in the 19th century by Cauchy. This method is implemented in many computer algebra systems (CAS), including Maple [8]. Although the formulation of the Cauchy method as such does not imply this, in all these implementations, the coefficients of the PDE are assumed to be given by unique analytical expressions throughout the entire considered domain. Therefore, to solve optical problems, it is necessary to develop new software capable of integrating first-order PDEs in the case when the coefficients of the equation are given by different analytical expressions in the subdomains G_1, \dots, G_k , into which the considered domain is divided.

This paper provides a mathematical description of this class of differential equations, offers the adaptation of the Cauchy integration method to this class of equations and its implementation as a Python program using the library SymPy [9].

1. Piecewise elementary partial differential equations

We restrict our consideration to some domain G in the space \mathbb{R}^n . We say that this domain is *divided into subdomains* G_1, \dots, G_k if two conditions are met:

- 1) the intersection of any pair of subdomains is empty, that is, $G_i \cap G_j = \emptyset$ ($i \neq j$),
- 2) the closure of the union of these domains gives the closure of G , i.e.,

$$\overline{G} = \overline{\cup G_i}.$$

We call such a partition *elementary*, if for any $i = 1, \dots, k$ we can specify an elementary expression g_i such that

$$G_i = \{x \in G : g_i(x) < 0\}.$$

The function f with the domain of definition G will be called given piecewise elementary if an elementary partition of the domain G into several subdomains is specified, and in each of these domains an elementary expression is given for f , i.e., an elementary partition G_1, \dots, G_k of the domain G and such elementary functions f_1, \dots, f_k exist such that

$$f|_{G_i} = f_i \quad \forall i = 1, \dots, k.$$

Now let x, y, z, p, q be five independent variables whose set of real values will be interpreted as a point in \mathbb{R}^5 . Let f be a piecewise elementary function defined in some domain G of this five-dimensional space. Then the expression

$$F(x, y, z, p, q) = 0, \tag{1}$$

where

$$p = \frac{\partial z}{\partial x}, \quad q = \frac{\partial z}{\partial y},$$

is a partial differential equation of the 1st order. We will refer to this kind of PDE as piecewise elementary.

The algorithm for integrating a first-order PDE is not related in any way with the form for specifying the differential equation and consists in finding the characteristics [6, 7]. Recall that characteristics are curves in the five-dimensional space $xyzpq$, which are integral curves for the characteristic system of ordinary differential equations (ODE) for characteristics, which is composed based on the given function F using arithmetic operations and differentiation:

$$\frac{dx}{F_p} = \frac{dy}{F_q} = \frac{dz}{p \cdot F_p + q \cdot F_q} = \frac{-dp}{F_x + p \cdot F_z} = \frac{-dq}{F_y + q \cdot F_z}, \quad (2)$$

where

$$F_x = \frac{\partial F}{\partial x}, \quad F_y = \frac{\partial F}{\partial y}, \quad F_z = \frac{\partial F}{\partial z}, \quad F_p = \frac{\partial F}{\partial p}, \quad F_q = \frac{\partial F}{\partial q}.$$

According to the well-known Cauchy theorem, a characteristic that intersects the plot of the solution of the equation (1) cannot leave this surface.

The 19th century authors integrated the ODE system (2) and using well-known integrals reconstructed the solution of PDE (1). Of course, the class of ODEs that are integrable in a symbolic form is very small [10], therefore, in modern CAS this system is solved numerically, thus combining numerical and analytical methods for integrating the PDE (1).

This technique can be described as follows. Let us know the curve C through which the desired solution of (1) should pass, and the value of p and q on the curve, or, equivalently, the curve in the space $xyzpq$, through which the manifold

$$z = f(x, y), \quad p = \frac{\partial f}{\partial x}(x, y), \quad q = \frac{\partial f}{\partial y}(x, y)$$

generated by the solution $z = f(x, y)$ of the considered PDE should pass. Then the desired solution of PDE is woven from the characteristics released from this curve. Replace the curve C with a broken line and from each of its vertices let out an integral curve, solving the initial problem for the characteristic system of ODE numerically, for example, according to the Runge–Kutta method. In this case, we will use the coordinates x, y, z of the vertex and the corresponding values of p and q as the initial data. In the general case, as a result, we get a network in the five-dimensional space $xyzpq$, the projection of which into the space xyz gives the skeleton of the surface, which approximates the graph of the exact solution. Therefore, the construction of this projection can complete an approximate solution of the PDE with the data on the curve C . Degeneration happens only when the curve C itself is a characteristic.

In the case when the PDE is piecewise elementary, it is necessary to make only a clarification in this scheme: when solving an ODE using the finite difference method, it is necessary at each step to find out to which domain the found point (x, y, z, p, q) of the integral curve belongs and to calculate the next point $(\hat{x}, \hat{y}, \hat{z}, \hat{p}, \hat{q})$ using the corresponding expression F_i instead of F .

Unfortunately, the standard functions built in computer algebra systems, e.g., in CAS Maple, do not allow this refinement of their algorithm, and are essentially useless in solving optical problems. Therefore, we wrote our implementation of this algorithm in the Python programming language using the SymPy [9] library. The code is laid out github.com [11] and is available under a free license. We called this package MF_Solver_PDE.

2. MF_Solver_PDE

Our software is focused on finding a solution to a piecewise elementary PDE (1) passing through the curve C in the space $xyzpq$.

The right side of the equation (1) is considered as a piecewise elementary function of five variables (x, y, z, p, q) . This means that the space $xyzpq$ is divided into several domains G_1, \dots, G_k , which are specified by inequalities $g_1 < 0, \dots, g_k < 0$. For each of these domains, the symbolic expressions F_1, \dots, F_k are given such that

$$F|_{G_i} = F_i \quad (i = 1, \dots, k).$$

Thus, to set the left-hand side of the equation (1) means to set the inequalities describing the domains G_1, \dots, G_k and the expressions F_1, \dots, F_k . In the SymPy package, like in any computer algebra system, we can work with such data types.

The input data for our algorithm for the solution of PDE are:

- the number k ;
- the inequalities describing domains G_1, \dots, G_k ;
- the expressions F_1, \dots, F_k ;
- the parametric representation for the curve C in \mathbb{R}^5 , through which the desired solution of PDE must pass.

The auxiliary parameters are:

- N , the number of points that will be taken on the curve C with an equal parameter step;
- h , the ODE discretisation step.

To find the PDE solution:

- 1) we find the coordinates of N points on the curve C ;
- 2) for each of them we form the initial problem of finding the characteristic that goes out of this point, and solve it using the Runge–Kutta method. We used the explicit fourth-order method with 4 stages [12, 13].

As a result of performing the described steps, a set of points in \mathbb{R}^5 is obtained, their projection into xyz space giving a set of points lying on the plot of the desired solution $z = z(x, y)$. By connecting with straight line segments the adjacent points lying on the same characteristic and the points found at the same step on two characteristics released from neighbouring points on the curve C , we get a two-dimensional skeleton of the surface. It can be turned into a surface plot using standard graphical tools available in SymPy.

3. Examples and verification

As the first example, consider the PDE

$$az = pq. \tag{3}$$

We will search for its solution passing through a straight line given parametrically in $xyzpq$ space $C : x = 1, y = \tau, z = b\tau, p = a\tau, q = b$.

This solution can be written explicitly as $z = (ax + b - a)y$.

The same solution obtained using our software is shown in Figure 1. The discrepancy between the numerical and analytical solutions is presented in Figure 2. It is clearly seen that the difference between numerical and analytical solutions is less than 10^{-7} and grows as the error is accumulated with each step.

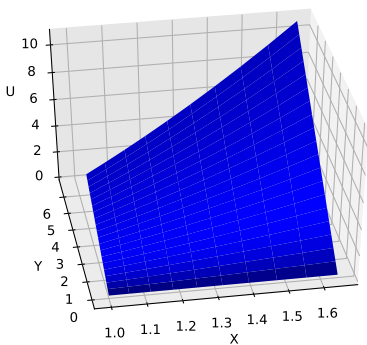


Figure 1. The solution of Eq. (3) using our software

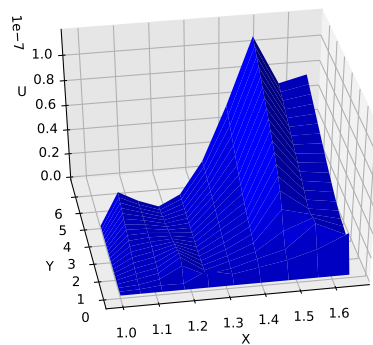


Figure 2. Discrepancy between numerical and analytical solutions of Eq. (3)

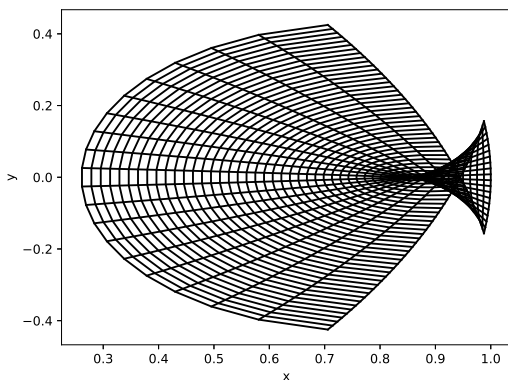


Figure 3. The surface describing the partial solution of the eikonal equation

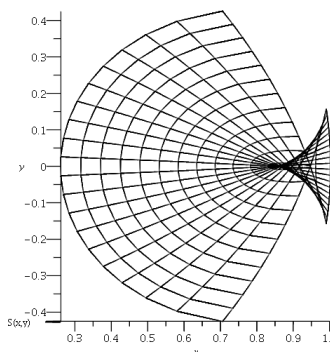


Figure 4. The surface describing the partial solution of the eikonal equation in the Maple program

As the second example, let us consider a problem from geometrical optics. The eikonal equation has the form $p^2 + q^2 = n^2(x, y)$.

Here n is the refractive index. Let for definiteness

$$n^2 = \begin{cases} 2 - x^2 - y^2, & x^2 + y^2 < 1, \\ 1, & x^2 + y^2 > 1. \end{cases}$$

In the present example, it is assumed that we have two domains: a circular Lüneburg lens and the medium in which it is placed (e.g., air) [14, 15]. The solution obtained using our software is demonstrated in Figure 3.

To check the correctness of the program work we compare the graphical solution, obtained using our program, with the Maple result. Certainly, in Maple the equations were solved only within the circle, and the boundary conditions have been chosen artificially. The Maple solution is shown in Figure 4. As seen from the figures, the solutions visually coincide.

Conclusion

The paper presents the original software for the numerical solution of first-order partial differential equations (PDE), the characteristic feature of which is that the coefficients of equations in different domains G_1, \dots, G_k are given by different analytical expressions F_1, \dots, F_k such that $F|_{G_i} = F_i \forall i = 1, \dots, k$.

The software was tested on benchmark problems taken from geometrical optics. A comparison with the results obtained by Maple was carried out.

The considered examples are illustrative. The software is potentially suitable for solving any first-order PDEs, the left-hand parts of which are piecewise described by very long symbolic expressions. Very complex equations of this type arise, for example, in the framework of the adiabatic waveguide method (AWM) proposed by A. A. Egorov and L. A. Sevastianov [3–5]. In this theory, the equation that plays the same role as the eikonal equation in geometrical optics is obtained by equating the determinant of a 8×8 matrix to zero. Even composing the symbolic expression for the right-hand side turns out to be a challenge for computer algebra systems. However, as soon as this expression is found, the proposed algorithm allows constructing the propagation of electromagnetic waves of the AWM in media with piecewise-specified refractive index. It is this application that we see as the natural scope of the software presented in this article.

Acknowledgments

The publication has been prepared with the support of the “RUDN University Program 5-100”.

References

1. M. Born, E. Wolf, Principles of optics. Electromagnetic theory of propagation, interference and diffraction of light, 6th Edition, Elsevier, 1980.
2. B. Enquist, O. Runborg, Computational high frequency wave propagation, 6th Edition, Cambridge University Press, 2003.

3. A. A. Egorov, L. A. Sevastianov, Structure of modes of a smoothly irregular integrated-optical four-layer three-dimensional waveguide, *Quantum Electronics* 39 (6) (2009) 566. doi:10.1070/QE2009v039n06ABEH013966.
4. A. A. Egorov, K. P. Lovetsky, L. A. Sevastianov, A. L. Sevastianov, Simulation of guided modes (eigenmodes) and synthesis of a thin-film generalised waveguide Luneburg lens in the zero-order vector approximation, *Quantum Electronics* 40 (9) (2010) 830–836. doi:10.1070/QE2010v040n09ABEH014332.
5. A. A. Egorov, L. A. Sevastianov, A. L. Sevastianov, Method of adiabatic modes in research of smoothly irregular integrated optical waveguides: zero approximation, *Quantum Electronics* 44 (2) (2014) 167–173. doi:10.1070/QE2014v044n02ABEH015303.
6. A. D. Polyandin, V. E. Nazaikinskii, *Handbook of linear partial differential equations for engineers and scientists*, 2nd Edition, CRC Press, Boca Raton, London, 2016.
7. E. Goursat, *Cours d'analyse mathématique*, 3rd Edition, Vol. 2, Gauthier-Villars, Paris, 1918.
8. PDEplot for Maple (2019).
URL <http://www.maplesoft.com>
9. Python library for symbolic mathematics SymPy (2019).
URL <http://www.sympy.org>
10. M. D. Malykh, On integration of the first order differential equations in finite terms, *IOP Conf. Series: Journal of Physics: Conf. Series* 788 (2017) 012026. doi:10.1088/1742-6596/788/1/012026.
11. IarKuz at Github (2019).
URL https://github.com/IarKuz/PostGradeCode/blob/MF_Solver_PDE/MF_Solver_PDE.ipynb
12. E. Hairer, G. Wanner, S. P. Nørsett, *Solving ordinary differential equations*, 3rd Edition, Vol. 1, Springer, New York, 2008.
13. W. H. Press, S. A. Teukolsky, W. T. Vetterling, B. P. Flannery, *Numerical recipes in C: the art of scientific computing*, 2nd Edition, Cambridge University Press, 1992.
14. J. Lock, Scattering of an electromagnetic plane wave by a Luneburg lens. II. Wave theory, *Journal of the Optical Society of America A: Optics Image Science and Vision* 25 (2008) 2980–2990. doi:10.1364/JOSAA.25.002980.
15. S. Cornbleet, Geometrical optics reviewed: A new light on an old subject, *Proceeding of the IEEE* 71 (1983). doi:10.1109/PROC.1983.12620.

For citation:

Ya. Yu. Kuziv, Software for the numerical solution of first-order partial differential equations, *Discrete and Continuous Models and Applied Computational Science* 27 (1) (2019) 42–48. DOI: 10.22363/2658-4670-2019-27-1-42-48.

Information about the authors:

Yaroslav Yu. Kuziv (Russian Federation) — postgraduate student of Department of Applied Probability and Informatics of Peoples' Friendship University of Russia (RUDN University) (e-mail: yaroslav.kuziw@yandex.ru, phone: +7(495)9550927)



Mathematical modeling

Research article

UDC 519.63

DOI: 10.22363/2658-4670-2019-27-1-49-59

Mathematical model of cavitation under the influence of a single stretching pulse

Nikolay Yu. Kravchenko¹, Dmitry S. Kulyabov²

¹ *Institute of Physical Research and Technology
Peoples' Friendship University of Russia (RUDN University)
6, Miklukho-Maklaya str., Moscow, 117198, Russian Federation*

² *Department of Applied Probability and Informatics
Peoples' Friendship University of Russia (RUDN University)
6, Miklukho-Maklaya str., Moscow, 117198, Russian Federation*

(received: August 6, 2019; accepted: October 21, 2019)

This paper describes the created mathematical model that allows you to explore the dynamics of cavitation bubbles under the influence of a single negative pressure pulse. The time dependence and coordinates of the parameters of the carrier phase, the temperature and pressure of the vapor phase, the concentration and size of the bubbles are determined numerically. It is concluded that the model created gives a good agreement between the calculated and experimental data.

Key words and phrases: numerical simulation, cavitation, mathematical model of cavitation

1. Introduction

Cavitation in a fluid is a process in which a dynamic decrease in pressure inside a fluid occurs at a constant temperature, as a result of which vapor and vapor-gas bubbles increase in the fluid caused by the evaporation of fluid into these bubbles. Bubbles (caverns) are formed in those places where the pressure in the liquid becomes below a certain critical value [1]. In a real fluid, it is approximately equal to the saturated vapor pressure at a given temperature [2].

Some features of cavitation

- Cavitation is peculiar only to liquids and does not occur under normal conditions, either in solids or in gases.

© Kravchenko N. Yu., Kulyabov D. S., 2019



This work is licensed under a Creative Commons Attribution 4.0 International License

<http://creativecommons.org/licenses/by/4.0/>

- Cavitation results from a decrease in pressure in a liquid, which means that it can be controlled by adjusting the pressure. If the pressure is maintained below a certain level for a long time, cavitation occurs.
- Cavitation is associated with the disappearance of cavities and their appearance in the liquid.
- Cavitation refers to non-stationary phenomena, since is a process of growth and collapse of cavities.
- Cavitation can occur both in the case of a moving fluid and in the case of a resting one.
- Cavitation can occur both in the volume of a liquid and on the solid boundary.

2. Cavitation equation

The equation describing the dynamics of cavitation bubbles in an incompressible fluid without taking into account the vapor pressure, surface tension and viscosity of the fluid can be represented as:

$$R\ddot{R} + \frac{3}{2}\dot{R}^2 = \frac{1}{\rho} \left[\left(p_b + \frac{2\sigma}{R_o} \right) \left(\frac{R_o}{R} \right)^{3k} - \frac{2\sigma}{R} - p_0 - p(t) \right]. \quad (1)$$

Here: R_0 is the radius of the nucleus at $t = 0$; R — radius of the nucleus at the next time instant t ; ρ — density of a liquid; σ is the surface tension of the fluid; $k = 1$ is the adiabatic index for steam in the bud; p_o is the hydrostatic pressure in a liquid ($p_o = p_b$); \ddot{R} is the acceleration of the cavity wall; \dot{R} is the speed of movement of the cavity wall; $2\sigma/R_0$ is the Laplace pressure; R_0/R is the amplitude of oscillations of the cavity.

3. Dynamics of a cavity under the action of single pulses of negative pressure

A single impulse is presented in the form:

$$p(t) = -\alpha (t + t_1) \exp \left(-\frac{t + t_1}{\tau} \right), \quad (2)$$

where t_1 is the time of appearance of the first germ of homogeneous cavitation under the action of this pulse.

In this case

$$\frac{dp}{dt} = \left(-\frac{1}{\tau} \right) \alpha (t + t_1) \exp \left(-\frac{t + t_1}{\tau} \right) + \alpha \exp \left(-\frac{t + t_1}{\tau} \right). \quad (3)$$

At $t = 0$, the rate of increase in pressure at the initial moment of time is $\alpha = -\frac{dp}{dt}$. From the condition $\frac{dp}{dt} = 0$, applied to (3) we find $t_m = \tau$, $p_m = \frac{\alpha\tau}{e}$, where τ is the rise time of the pressure pulse up to the maximum value p_m . Let us set the maximum pressure amplitude p_m so that it approaches 95% to the thermodynamic stability [3] of the fluid (spinodal, [4]), i.e.

$$p_m = 0.95(p_b - p_s). \quad (4)$$

Then from (4) it follows that

$$\alpha = \frac{1}{\tau} 0.95e(p_b - p_s). \quad (5)$$

Thus, the rate of pressure increase α can be calculated for a given fluid temperature using the value of $(p_b - p_s)$ for a given τ .

The time of appearance of the first nucleus t_1 is found from the condition (2), when at $t = t_1$ the pressure is $p = p_1$.

$$p_1 = -\alpha t_1 \cdot \exp\left(-\frac{t_1}{\tau}\right) = -\beta(p_b - p_s). \quad (6)$$

Here p_1 is the pressure at which one germ appears in 1 cm^3 at the moment of time t_1 ,

$$\beta = -\frac{p_1}{p_b - p_s} < 1. \quad (7)$$

Substituting α into (6), we get

$$\beta = e \cdot \frac{t_1}{\tau} \cdot \exp\left(-\frac{t_1}{\tau}\right) = e \cdot x \cdot \exp(-x) \quad (8)$$

where $x = t_1/\tau$.

Thus, in the equation (3), for a given value of τ , the value of α ; is calculated by the formula (5) and the value of t_1 is calculated by the formula (2) for a given value of β (formula (8)).

To determine the time t_1 , it is necessary to take into account the number of bubbles appearing per unit of time per unit volume of liquid:

$$\frac{dN}{V \cdot dt} = B \cdot \exp\left[-\frac{16\pi\sigma^3}{3(1 - \rho_v/\rho_l)^2(p_b - p)^2}\right],$$

$$V = 1 \text{ sm}^3,$$

$$A = \frac{16\pi\sigma^3}{3(1 - \rho_v/\rho_l)^2}, \quad (9)$$

$$p_b - p = \alpha t,$$

$$dN = B \cdot \exp\left(-\frac{A}{\alpha^2 t^2}\right) dt,$$

$$N = 1 = B \int_0^{t_1} \exp\left(-\frac{A}{\alpha^2 t^2}\right) dt. \quad (10)$$

By calculating α and A through the formulae (9) and (10) by integrating respectively and assuming that $B \approx 10^{33} \text{ cm}^{-3} \text{ s}^{-1}$ at $N = 1$ the time t_1 is calculated.

Denoting by

$$C = -\frac{A}{\alpha^2},$$

we get that

$$B \cdot \int_0^{t_1} \exp\left(\frac{C}{t^2}\right) dt = 1. \quad (11)$$

Taking into account the geometric meaning of a definite integral (11), one can determine the point t_1 , by numerical method knowing that the area of the figure bounded by the function $f(x)$ on the interval $[0, t_1]$ should be equal to 1.

In the basic cavitation equation (1), we substitute the expression for pressure in the form (2). Then the basic cavitation equation (Rayleigh equation) takes the form:

$$R\ddot{R} + \frac{3}{2}\dot{R}^2 = \frac{1}{\rho} \left[\left(p_b + \frac{2\sigma}{R_o} \right) \left(\frac{R_o}{R} \right)^{3k} - \frac{2\sigma}{R} - p_b - \alpha (t + t_1) \exp\left(-\frac{t + t_1}{\tau}\right) \right]. \quad (12)$$

The differential equation for the growth of an embryo vapor has the form:

$$\rho_l \left(R\ddot{R} + \frac{3}{2}\dot{R}^2 \right) = -p(t) - \frac{2\sigma}{R} \left(1 - \frac{\rho_l}{\rho_v} \right)^{-1}, \quad (13)$$

where $p(t)$ is defined by the formula (2).

Substituting $p(t)$ from (2) into (13), we get:

$$\rho_l \left(R\ddot{R} + \frac{3}{2}\dot{R}^2 \right) = \alpha(t + t_1) \cdot \exp\left(-\frac{t + t_1}{\tau}\right) - \frac{2\sigma}{R} \left(1 - \frac{\rho_l}{\rho_v} \right)^{-1}. \quad (14)$$

For the reasons described above, we will assume $t_1 \approx 0$, and then the equation (14) takes the form:

$$\rho_l \left(R\ddot{R} + \frac{3}{2}\dot{R}^2 \right) = \alpha \cdot t \cdot \exp\left(-\frac{t}{\tau}\right) - \frac{2\sigma}{R} \left(1 - \frac{\rho_l}{\rho_v} \right)^{-1}. \quad (15)$$

It is solved by us numerically. For this, it is necessary to present the last equation in the form of a system of two equations in which the following

change of variables is introduced:

$$\begin{aligned} R &= u(2), \\ \dot{R} &= du(2) = u(1), \\ \ddot{R} &= du(1). \end{aligned}$$

The equation (15) by changing variables is converted to the form:

$$\ddot{R} = \frac{1}{\rho_l R} \left[\alpha t \exp\left(-\frac{t}{\tau}\right) - \frac{2\sigma}{R} \left(1 - \frac{\rho_l}{\rho_v}\right)^{-1} \right] - \frac{3}{2} \frac{\dot{R}^2}{R \rho_l} \quad (16)$$

or

$$du(1) = \frac{1}{\rho_l u(2)} \left[\alpha t \exp\left(-\frac{t}{\tau}\right) - \frac{2\sigma}{u(2)} \left(1 - \frac{\rho_l}{\rho_v}\right)^{-1} \right] - \frac{3}{2} \frac{[u(1)]^2}{u(2) \rho_l}. \quad (17)$$

The last equation is solved numerically by the Runge–Kutta method. The calculations were carried out for $\tau = 10^{-9}$ s.

It was believed that at the initial time, a homogeneous liquid that does not contain vapor bubbles was at a given temperature and pressure

$$t = 0, \quad p_l = p_{l0}, \quad T_l = T_{l0}, \quad N_b = 0, \quad u = 0.$$

The rate of pressure drop α_p at the point with coordinate $x = 0$ was set by the boundary conditions

$$x = 0, \quad p_l = p_{l0} - \alpha_p \cdot t, \quad \frac{\partial u}{\partial x} = 0.$$

After a bubble appeared, the following initial conditions were accepted for ordinary differential equations describing its development (12): $R = R_c$, $p_v = p_b$, $t_v = T_l$.

4. Method of numerical solution of the equation

We introduce the following notation, convenient for working with the program for the numerical solution of the basic cavitation equation in the form (1):

$$\begin{aligned} \omega R_0 &= omr0, \quad \frac{2\sigma}{R_0} = sr0, \quad P_b = pb, \\ (\omega R_0)^2 &= omr02, \quad \left(P_b + \frac{2\sigma}{R_0}\right) = pbsr0, \quad P_a = pa, \\ \rho(\omega R_0)^2 &= rhomr, \quad \varphi_o = fio, \quad R^* = u(2), \quad z^* = u(1). \end{aligned}$$

Then the original equation (1) takes the form of a system of two first order differential equations:

$$\begin{cases} du(1) = -\frac{3}{2} \frac{1}{omr0} \frac{u(1)}{u(2)} + \\ \quad + \frac{1}{rhomr} \frac{1}{u(2)} \left[\frac{pbsr0}{(u(2))^{3k}} - sr0 \frac{1}{u(2)} - pb + pa \cdot \sin(\tau + fio) \right], \\ du(2) = u(1). \end{cases}$$

The resulting system of differential equations is solved numerically by the Runge–Kutta method. It should be noted that numerical solutions were cited earlier for other cases [5–9].

5. The program for the numerical solution

We have created a program for the numerical solution of the cavitation equation in the *Compaq Visual Fortran Professional* programming language. Its work is based on the Runge–Kutta method.

Initially, the main program asks for the values of external parameters, such as fluid temperature, oscillation frequency, and others (see Fig. 1). Then the main program refers to an array of tabular data for the values of surface tension, fluid viscosity, fluid pressure, vapor pressure at a given temperature. These tabular data are discrete values and do not always correspond to a given temperature. Therefore, the main program refers to auxiliary subroutine 1, which approximates or extrapolates the table data to a given point.

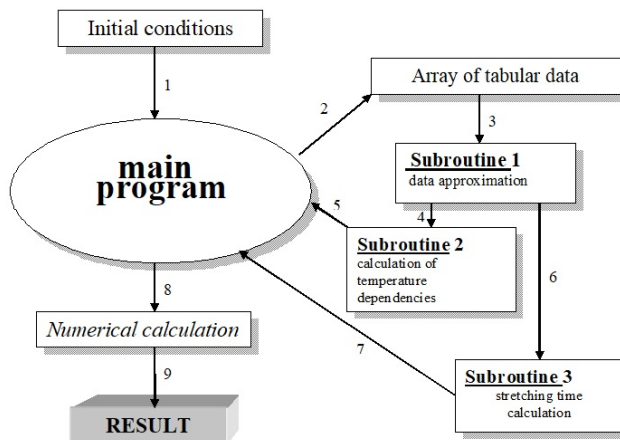


Figure 1. Block diagram

To calculate parameters such as the initial radius of the cavity, the pressure at which the first cavitation nucleus appears, the initial phase of external oscillations, the main program refers to subroutine 2, which calculates these values based on the data already calculated by subroutine 1.

Subroutine 3 then receives from subprogram 2 a task to calculate the time t_1 during which the first cavitation nucleus appears in the fluid. The required

tabular data is requested from subroutine 1. The result of the calculation is reported to the main program.

Having collected all the necessary data, the main program calculates the basic cavitation equation for the maximum amplitude of oscillations of the cavity in case of acoustic cavitation [10,11]. It should be noted that this case is also interesting in the possibility of initiating a nuclear fusion reaction [12–14], which is confirmed by the theory [15,16].

Below is a part of the main program for the numerical solution of this system of equations, written in the programming language *Fortran*:

```

external rad,res
dimension pt(5), u(2), du(2), aux(8,2)
common omr0, rmr0, rhomr, pbsr0, pk, sr0, pa, pb, pi, nk,
  → fa, r0, p, p1, fi0, ky
open(1, file='p.dat')
open(2, file='r.dat')
open(3, file='bubble.txt')
print *, 'The program for calculating the dynamics of the
  → bubble with acoustic effects and the frequency of Fa
  → according to Runge Kutta method.'
print *, '-----'
print *, 'time pressure dependence  $P = P(t / T)$  is
  → written to the file "p.dat", the time dependence of
  → the radius  $R / R_0 = f(t / T)$  is written to the file
  → "r.dat".'
print *, 'THE PROGRAM WILL NOT WORK without an auxiliary
  → file "bubble.txt" and also without the additional
  → program "rkgs.for"!'
read (3, *) q1, q2, fa, pa, pb, p1, r0, sig, amu, ro, kt,
  → ky
pi = 3.141592654
pk = 5
print *, 'The following parameters are entered here:'
print *, '1) Time step integration (wt): pt (3) =', q1
print *, '2) Integration error: pt (4) =', q2
print *, '3) Acoustic frequency: Fa =', fa, 'Hz'
print *, '4) Pressure amplitude at a given point: Pa =',
  → pa, 'Pa'
print *, '5) Pressure on binodals at a given point: Pb =',
  → pb, 'Pa'
print *, '6) Pressure at the point of emergence of the
  → unit: P1 =', p1, 'Pa'
print *, '7) Starting radius of the nucleus: R0 =', r0,
  → 'm'
print *, '8) Surface tension: sigma =', sig, 'N / m'
print *, '9) Molar mass: mu =', amu, 'kg / mol'
print *, '10) The density of the fluid at this point: po
  → =', ro, 'kg / m * 3'
print *, '11) Number of periods studied: n =', kt
print *, '12) Number of points for one period: N =', ky
print *, ''

```

```

print *, 'Changing these parameters is possible only in
→ the file' bubble.txt ''
print *, 'To interrupt the program, press "Ctrl + C", for
→ continuation - "Enter"'
pause
om=2.0*pi*fa
omr0=om*r0
omr02=omr0*omr0
rhomr=ro*omr02
rmr0=4.*amu/(r0*ro)
sr0=2.*sig/r0
fi0=asin((pb-p1)/pa)
pbsr0=pb+sr0
pt(1)=0.0
pt(2)=2.0*pi*kt
nk=1
6  continue
pt(3)=q1
pt(4)=q2
u(1)=0.0
u(2)=1.
du(1)=0.5
du(2)=0.5
call rkgs (pt,u,du,2,ih,rad,res,aux)
if(ih-10)3,3,4
3  continue
print *, ' Error code ',ih
goto 5
4  continue
print *, '
print *, '          ATTENTION   !!!'
print *, 'ERROR CODE SHOULD NOT EXCEED 10.'
print *, 'Correct, please, the parameters pt(3),pt(4)'
read(*,*)q1,q2
goto 6
5  continue
stop
end

```

Below are some results of a numerical simulation of the bubble behavior in a rarefaction wave.

6. Conclusions

The mathematical model created by us allows us to investigate the dynamics of cavitation bubbles with a change in fluid pressure. Numerical simulation made it possible to determine the time dependence and coordinates of the parameters of the carrier phase, the temperature and pressure of the vapor phase [17], the concentration and size of the bubbles. The proposed model is applicable not only to liquids, but also to metals in the liquid phase [18].

We concluded that the model created gives a good agreement between the calculated and experimental data [19], which demonstrates the applicability of the approach under consideration to the problem of rapid pressure drop.

In the studied problem, the following picture takes place: the pressure of the fluid drops in the rarefaction wave to a value below the saturation pressure, the fluid enters a metastable state [20], intense nucleation begins in the region of minimal pressure, after which the bubbles rapidly increase due to the interfacial mass transfer, which ultimately account stabilizes the pressure at a value close to the saturation pressure.

Acknowledgments

The publication has been prepared with the support of the “RUDN University Program 5-100”.

References

1. N. Yu. Kravchenko, M. M. Martynyuk, Dynamics of homogeneous cavitation bubbles in water under large amplitude pressure oscillations, *Bulletin of Peoples' Friendship University of Russia. Series: Physics* 8 (2000) 118–121, in Russian.
2. A. A. Aganina, M. A. Ilgamov, D. Yu. Toporkova, Dependence of vapor compression in cavitation bubbles in water and benzol on liquid pressure, *Proceedings of Kazan University. Physics and Mathematics Series [Uchenye zapiski kazanskogo universiteta. Seriya fiziko-matematicheskie nauki]* 158 (2) (2016) 231–242.
URL <http://mi.mathnet.ru/eng/uzku1365>
3. M. M. Martynyuk, N. Yu. Kravchenko, Limit of thermodynamic stability of a liquid phase in the field of negative pressure [Granitsa termodinamicheskoy ustoychivosti zhidkoy fazy v oblasti otritsatel'nykh davleniy], *Russian Journal of Physical Chemistry* 72 (6) (1998) 998–1001, in Russian.
4. P. A. Tamanga, M. M. Martynyuk, N. Yu. Kravchenko, Spinodal of liquid phase on basis of generalized berthelo's equation, *Bulletin of Peoples' Friendship University of Russia. Series: Physics* (9) (2001) 56–58, in Russian.
5. N. Yu. Kravchenko, The numerical solution of the Rayleigh-Plisset equation for spark cavitation and calculation of the maximum temperature and pressure in a cavity, *Journal of Mechanics of Continua and Mathematical Sciences (Special Issue-1)* (2019) 465–473. doi:10.26782/jm-cms.2019.03.00046.
6. E. V. Butyugina, E. S. Nasibullaeva, Numerical study of the gas diffusion process between clustered bubbles and technical fluids [Issledovaniye protsessa diffuzii gaza mezhdru puzyr'kom v klasteri i tekhnicheskoy zhidkost'yu], *News of the Ufa Scientific Center [Izvestiya UNTS RAN]* (2) (2016) 15–21, in Russian.
7. A. B. Kapranova, A. E. Lebedev, A. M. Meltser, S. V. Neklyudov, S. E. M., Methods of modeling the developmental stages of hydrodynamic cavitation, *Fundamental Research [Fundamental'nyye issledovaniya]* (3) (2016) 268–273, in Russian.

8. Modelling of cavitation and bubble growth during ultrasonic cleaning process, in: T. Sile, J. Virbulis, A. Timuhins, J. Sennikovs, U. Bethers (Eds.), Proc. of International Scientific Colloquium Modelling for Material Processing, September 16-17, Riga, Latvia, 2010, pp. 329–334.
9. E. V. Volkova, E. S. Nasibullaeva, N. A. Gumerov, Numerical simulations of soluble bubble dynamics in acoustic fields, in: Proc. of the ASME 2012 International Mechanical Engineering Congress & Exposition (IMECE 2012), Houston, Texas, USA, 2012, pp. 317–323, 1 CD ROM.
10. A. A. Gubaydullin, A. C. Gubkin, Behavior of bubbles in cluster with acoustic exposure [Povedeniye puzyr'kov v klasterie pri akusticheskom vozdeystvii], Modern Science. Researches, Ideas, Results, Technologies (1 (12)) (2013) 363–367, in Russian.
11. E. V. Butyugina, E. S. Nasibullaeva, N. A. Gumerov, I. S. Akhatov, Numerical simulation of gas microbubble dynamics in an acoustic field with account for rectified diffusion [Chislennoye modelirovaniye dinamiki gazovogo mikropuzyr'ka v akusticheskom pole s uchetom protsessy napravlennoy diffuzii], Vychislitel'naya mekhanika sploshnykh sred 7 (3) (2014) 234–244, in Russian.
12. R. P. Taleyarkhan, C. D. West, J. S. Cho, R. T. Lahey Jr., R. I. Nigmatulin, R. C. Block, Evidence for nuclear emissions during acoustic cavitation, *Science* 295 (2002) 1868–1873. doi:10.1126/science.1067589.
13. R. P. Taleyarkhan, C. D. West, R. T. Lahey Jr., R. I. Nigmatulin, R. C. Block, Y. Xu, Nuclear emissions during self-nucleated acoustic cavitation, *Physical Review Letters* 96 (2006). doi:10.1103/PhysRevLett.96.034301.
14. M. M. Martynyuk, N. Yu. Kravchenko, Nuclear fusion reaction in mataphase substance in the process of electrical explosion [Reaktsii yadernogo sinteza v mezofaznom veshchestve v protsesse elektricheskogo vzryva], *Applied Physics* (1) (2003) 79–90, in Russian.
15. R. I. Nigmatulin, I. S. Akhatov, A. S. Topolnikov, R. K. Bolotnova, N. K. Vakhitova, R. T. Lahey Jr., R. P. Taleyarkhan, The theory of supercompression of vapor bubbles and nano-scale thermonuclear fusion, *Phys. Fluids* 17 (10) (2005) 1–31, art. 107106. doi:10.1063/1.2104556.
16. M. M. Martynyuk, N. Yu. Kravchenko, Impact-cluster nuclear fusion. Conditions of excitation of the process, *Bulletin of Peoples' Friendship University of Russia. Series: Physics* (1) (2005) 118–128, in Russian.
17. Determination of temperature and pressure within the cavitation cavity [Opredeleniye temperatury i davleniya vnutri kavitatsionnoy polosti], in Russian.
18. M. M. Martynyuk, P. A. Tamanga, N. Yu. Kravchenko, The titanium phase diagram at the phase transition region liquid-vapor, *Bulletin of Peoples' Friendship University of Russia. Series: Physics* (10) (2002) 121–125, in Russian.
19. V. N. Khmelev, S. S. Khmelev, R. N. Golykh, G. A. Bobrova, O. N. Krasulja, V. I. Bogush, S. Anandan, Experimental determining of conditions of ultrasonic influence for providing maximum cavitation intensity in medium [Eksperimental'noye opredeleniye usloviy ul'trazvukovogo vozdeystviya dlya obespecheniya maksimal'noy intensivnosti kavitatsii v srede], *Yuzhno-Sibirskiy nauchnyy vestnik* (4 (12)) (2015) 50–55, in Russian.

20. A. A. Aganin, Dynamics of a small bubble in a compressible fluid, *International Journal for Numerical Methods in Fluids* 33 (2) (2000) 157–174. doi:10.1002/(SICI)1097-0363(20000530)33:2<157::AID-FLD6>3.0.CO;2-A.

For citation:

N. Yu. Kravchenko, D. S. Kulyabov, Mathematical model of cavitation under the influence of a single stretching pulse, *Discrete and Continuous Models and Applied Computational Science* 27 (1) (2019) 49–59. DOI: 10.22363/2658-4670-2019-27-1-49-59.

Information about the authors:

Nikolay Yu. Kravchenko (Russian Federation) — Deputy Director of Institute of Physical Research and Technology, Peoples' Friendship University of Russia (RUDN University) (e-mail: kravchenko-nyu@rudn.ru, phone: +7(495)9550839, ORCID: <https://orcid.org/0000-0003-3397-1746>, ResearcherID: E-6162-2018, Scopus Author ID: 14633789300)

Dmitry S. Kulyabov (Russian Federation) — Doctor of Sciences in Physics and Mathematics, Full Professor, Department of Applied Probability and Informatics, Peoples' Friendship University of Russia (RUDN University), (e-mail: kulyabov-ds@rudn.ru, phone: +7(495)9520250, ORCID: <https://orcid.org/0000-0002-0877-7063>, ResearcherID: I-3183-2013, Scopus Author ID: 35194130800)



UDC 519.644

DOI: 10.22363/2658-4670-2019-27-1-60-69

The volume integral equation method in magnetostatic problem

Pavel G. Akishin, Andrey A. Sapozhnikov

*Joint Institute for Nuclear Research
6 Joliot-Curie str, Dubna, Moscow region, 141980, Russian Federation*

(received: February 22, 2019; accepted: October 21, 2019)

This article addresses the issues of volume integral equation method application to magnetic system calculations. The main advantage of this approach is that in this case finding the solution of equations is reduced to the area filled with ferromagnetic. The difficulty of applying the method is connected with kernel singularity of integral equations. For this reason in collocation method only piecewise constant approximation of unknown variables is used within the limits of fragmentation elements inside the famous package GFUN3D. As an alternative approach the points of observation can be replaced by integration over fragmentation element, which allows to use approximation of unknown variables of a higher order.

In the presented work the main aspects of applying this approach to magnetic systems modelling are discussed on the example of linear approximation of unknown variables: discretisation of initial equations, decomposition of the calculation area to elements, calculation of discretised system matrix elements, solving the resulting non-linear equation system. In the framework of finite element method the calculation area is divided into a set of tetrahedrons. At the beginning the initial area is approximated by a combination of macro-blocks with a previously constructed two-dimensional mesh at their borders. After that for each macro-block separately the procedure of tetrahedron mesh construction is performed. While calculating matrix elements sixfold integrals over two tetrahedra are reduced to a combination of fourfold integrals over triangles, which are calculated using cubature formulas. Reduction of singular integrals to the combination of the regular integrals is proposed with the methods based on the concept of homogeneous functions. Simple iteration methods are used to solve non-linear discretized systems, allowing to avoid reversing large-scale matrixes. The results of the modelling are compared with the calculations obtained using other methods.

Key words and phrases: finite element method, magnetostatics, volume integral equations, systems of nonlinear equations, cubature formulae, iterative process

Introduction

The paper [1] gives an overview of existing methods and programs for the numerical simulation of magnetic systems. The issues concerning the volume

© Akishin P. G., Sapozhnikov A. A., 2019



This work is licensed under a Creative Commons Attribution 4.0 International License

<http://creativecommons.org/licenses/by/4.0/>

integral equation method [2–5] for magnetic system calculations are discussed in this article. We consider the approach, which allows to construct high order accuracy approximation method for initial problem discretization. The main steps of the modelling process are being discussed: discretization of the initial equations for linear approximation of the magnetic field, algorithm of area division into elements, matrix element calculation procedures, a method of solving a corresponding system of nonlinear equations. The numerical results obtained for the modelling of quadrupole and dipole magnet agree with those obtained by the famous code TOSCA [6].

1. Volume integral equation method

Let $\bar{B}(\bar{a})$, $\bar{H}(\bar{a})$, $\bar{M}(\bar{a})$ be the induction, the intensity and the magnetization of the magnetic field at the point \bar{a} . The values \bar{B} , \bar{H} , \bar{M} are connected by the following nonlinear ratios [7]:

$$\bar{H}(\bar{a}) = \frac{\bar{B}(\bar{a})}{\mu (|\bar{B}(\bar{a})|) \mu_0}, \quad \bar{M}(\bar{a}) = \frac{\bar{B}(\bar{a})}{\mu_0} - H(\bar{a}), \quad (1)$$

where μ_0 is the absolute magnetic permeability of vacuum; $\mu(x)$ is the magnetic permeability. The following integral equation is true:

$$\bar{H}(\bar{a}) = \bar{H}^S(\bar{a}) + \frac{1}{4\pi} \nabla_{\bar{a}} \int_G \left(\bar{M}(\bar{x}), \nabla_{\bar{a}} \frac{1}{|\bar{x} - \bar{a}|} \right) dv_{\bar{x}},$$

where $\bar{H}^S(\bar{a})$ is the magnetic field from the current winding. G is the area filled with iron. The field $\bar{H}^S(\bar{a})$ can be found according to the Biot–Savart law [8]:

$$\bar{H}^S(\bar{a}) = \frac{1}{4\pi} \text{Rot}_{\bar{a}} \int_{R^3} \frac{\bar{J}(\bar{x})}{|\bar{x} - \bar{a}|} dv_{\bar{x}},$$

where $\bar{J}(\bar{x})$ is current density. The difficulty of applying the integral approach is related to the singularity of the kernel of the integral equations.

This is the reason why only a piecewise approximation of unknown parameters within division element area is used in GFUN3D code [2]. Alternatively to collocation method, integration over dividing elements can be used.

It allows to use higher order approximation for unknown variables. The most convenient mathematical approach for constructing such type of approximations is the finite element method (FEM) [9–12].

Let us divide area G into tetrahedrons $\{G_i\}$. We suppose that the fragmentation $G = \bigcup_{i=1}^N G_i$ satisfies the requirements of FEM. Let us assume $\{\bar{P}_k, k = 1, \dots, L\}$ is the set of all vertexes in all tetrahedrons $\{G_i\}$. Let us introduce the notation $\bar{B}_k = \bar{B}(\bar{P}_k)$, $\bar{H}_k = \bar{H}(\bar{P}_k)$, $\bar{M}_k = \bar{M}(\bar{P}_k)$. We denote $f_k(\bar{x})$ — as a node function, associated with vertex \bar{P}_k . The functions $f_k(\bar{x})$ on each tetrahedron are linear functions, equaled to 1 at the vertex \bar{P}_k and to 0

at any other vertexes. Using these notations we define linear approximations for vectors $\bar{B}(\bar{a})$, $\bar{H}(\bar{a})$, $\bar{M}(\bar{a})$:

$$\hat{B}(\bar{a}) = \sum_{k=1}^L f_k(\bar{a})\bar{B}_k, \quad \hat{H}(\bar{a}) = \sum_{k=1}^L f_k(\bar{a})\bar{H}_k, \quad \hat{M}(\bar{a}) = \sum_{k=1}^L f_k(\bar{a})\bar{M}_k.$$

We characterize a discretized formulation of magnetostatic problem, using the finite element linear approximation within division elements [13]:

$$\begin{aligned} \sum_{j=1}^L \int_G f_i(\bar{a})f_j(\bar{a})\bar{H}_j dv_{\bar{a}} &= \int_G f_i(\bar{a})\bar{H}^S(\bar{a}) dv_{\bar{a}} + \\ &+ \sum_{j=1}^L \int_G f_i(\bar{a}) \frac{\nabla_a}{4\pi} \left[\int_G f_j(\bar{x}) \left(\bar{M}_j, \nabla_a \frac{1}{|\bar{x} - \bar{a}|} \right) dv_{\bar{x}} \right] dv_{\bar{a}}, \quad i = \overline{1, L}. \end{aligned} \quad (2)$$

Let matrix $[C]$ be a matrix of $[3L \times 3L]$:

$$[C] = \begin{bmatrix} [C_{11}] & \cdots & [C_{1L}] \\ \vdots & \ddots & \vdots \\ [C_{L1}] & \cdots & [C_{LL}] \end{bmatrix},$$

where $[C_{ij}]$ — is a diagonal matrix of $[3 \times 3]$ dimension such as

$$[C_{ij}] = \int_G f_i(\bar{a})f_j(\bar{a}) dv_{\bar{a}} \begin{pmatrix} 1 & 0 & 0 \\ 0 & 1 & 0 \\ 0 & 0 & 1 \end{pmatrix}.$$

Let $[A]$ be a matrix of $[3L \times 3L]$ dimension:

$$[A] = \begin{bmatrix} [A_{11}] & \cdots & [A_{1L}] \\ \vdots & \ddots & \vdots \\ [A_{L1}] & \cdots & [A_{LL}] \end{bmatrix},$$

where $[A_{ij}]$ — is a matrix of $[3 \times 3]$ dimension, such as for any constant vector \bar{M} the following ratio is true:

$$[A_{ij}]\bar{M} = \int_G f_i(\bar{a}) dv_{\bar{a}} \frac{\nabla_a}{4\pi} \left[\int_G f_j(\bar{x}) \left(\bar{M}, \nabla_a \frac{1}{|\bar{x} - \bar{a}|} \right) dv_{\bar{x}} \right]. \quad (3)$$

Let the following be true:

$$\hat{B} = (\bar{B}_1, \bar{B}_2, \dots, \bar{B}_L)^T,$$

$$\hat{M}(\hat{B}) = (\mu_0 \bar{M}(\bar{B}_1), \mu_0 \bar{M}(\bar{B}_2), \dots, \mu_0 \bar{M}(\bar{B}_L))^T,$$

$$\hat{H}^S = \left(\mu_0 \int_G f_1(\bar{a}) \bar{H}^S(\bar{a}) dv_{\bar{a}}, \mu_0 \int_G f_2(\bar{a}) \bar{H}^S(\bar{a}) dv_{\bar{a}}, \dots, \mu_0 \int_G f_L(\bar{a}) \bar{H}^S(\bar{a}) dv_{\bar{a}} \right)^T.$$

Taking into account (1), the system (2) could be written in the following way:

$$[C] \hat{B} = \hat{H}^S + ([A] + [C]) \hat{M}(\hat{B}). \quad (4)$$

Using node functions of higher order similarly to (2) it is possible to formulate a discretization with quadratic, cubical or higher approximation of variables within the element.

2. Finite element mesh generating

In order to build a discretization for the integral equations (2) the region of calculations should be divided into the tetrahedrons, satisfying the requirements of FEM. There are many articles dedicated to this problem [14–17]. Depending on the task, there are different requirements for mesh elements. In subregions, where the solution should change faster, more detailed discretization is needed, and as a result, the element size must be smaller. And, vice versa, within the regions of slow solution changing, detailed division leads to a big number of elements, thus complicating the solving of the final discretized system of equations. That is why in such regions the element size must be larger. Moreover, the final mesh elements should not be degenerated. The degenerated elements affect the solution approximation and the convergence of iterative methods, used for solving the discretized problem. In the case of constructing mesh with heterogeneous materials there are additional restraints for a division related to medium edge borders. These borders usually look like curves on a plain or surfaces in space and should not be crossed by the edge of the mesh. In fact, these limitations show that every element of the mesh should consist of only one particular substance. The region edges can be approximated with lines or surfaces as well as with curves and second or further order surfaces. Such edges are approximated with resultant elements according to the size of the considered mesh sub-region.

In report [18] the problems of multidimensional finite element mesh generation based on electromagnetic fields modelling in large-scale electromagnetic machines have been discussed. A description of the three-dimensional adaptive mesh generator **3DFEMMesh**, a review of mesh generation methods and a number of the existing criteria for a quality assessment of the constructed mesh are given in this work. The procedure of mesh construction is based on a representation of the problem domain as a combination of standard 3D macroblocks. After generating of a two-dimensional mesh on all macroblocks boundaries, three-dimensional mesh in each block may be constructed individually. The program has a graphical interface for the data entry and a visual assessment of the partition quality. The generator **3DFEMMesh** is included into JINR programme library **JINRLIB** [19].

3. Matrix element calculation

The problem of defining matrix coefficients of the discretized equations can be reduced to calculating sixfold, singular in general case, integrals from (3) by two tetrahedrons. The simplest way to evaluate these integrals is to use a cubature. Given a big number of integrals to be calculated, requirements to cubature formula optimality are extremely important. Because of singularity of the function being integrated the necessity of using cubature formula of high accuracy arises [20]. In monograph [21] the issues of the general theory of cubature formula building are studied and many cubature formulas for different types of simplexes are listed. While calculating integrals, which are necessary for the discretized equations, there might be situations when the integrated function is singular. Moreover, there are situations when the function being integrated is singular in every point of the volume under integration. In those cases cubature formula application is not possible and we need to develop further methods for such kind of integration.

First of all, we consider the method which allows to decrease the coefficient calculation time of the discretized systems. The matrix coefficients in $[A_{ij}]$ from (3) can be presented as sum of integrals such as:

$$J_{m,i,k}^{n,j,l} = \int_{G_m} \int_{G_n} \left[f_i(\bar{x}) f_j(\bar{a}) \frac{\partial^2}{\partial x_k \partial a_l} \frac{1}{|\bar{x} - \bar{a}|} \right] dv_{\bar{x}} dv_{\bar{a}}.$$

Taking into account that $\{f_k(\bar{x})\}$ are linear functions and, as a consequence, the function gradient vectors are constant inside each tetrahedron, such volume integrals can be reduced to surface integrals thus:

$$\begin{aligned} J_{m,i,k}^{n,j,l} = & \oint_{\partial G_m} \oint_{\partial G_n} \frac{f_i(\bar{x}) f_j(\bar{a}) (d\bar{S}_x, \bar{e}_k) (d\bar{S}_a, \bar{e}_l)}{|\bar{x} - \bar{a}|} - \\ & - 0.5 \frac{\partial f_i^m(\bar{x})}{\partial x_k} \frac{\partial f_j^n(\bar{a})}{\partial a_l} \oint_{\partial G_m} \oint_{\partial G_n} \frac{(d\bar{S}_x, d\bar{S}_a)}{|\bar{x} - \bar{a}|} - \\ & - 0.5 \frac{\partial f_i^m(\bar{x})}{\partial x_k} \oint_{\partial G_m} \oint_{\partial G_n} f_j(\bar{a}) (dS_a, \bar{e}_l) \frac{((\bar{x} - \bar{a}), d\bar{S}_x)}{|\bar{x} - \bar{a}|} - \\ & - 0.5 \frac{\partial f_j^n(\bar{a})}{\partial a_l} \oint_{\partial G_m} \oint_{\partial G_n} f_i(\bar{x}) (dS_x, \bar{e}_k) \frac{((\bar{a} - \bar{x}), d\bar{S}_a)}{|\bar{a} - \bar{x}|}, \quad (5) \end{aligned}$$

where \bar{e}_k, \bar{e}_l are unit coordinate system vectors.

The notation $\partial f_i^m(\bar{x})/\partial x_k$ means that the derivative is calculated on the tetrahedron G_m . It is important to note that region G consists of a union of tetrahedrons. Then the borders $\{\partial G\}$ are triangles. Thus, calculating the expressions (5) reduces a 6D integral to a sum of 4D integrals over two triangles. There are four types of the positional relationships of triangles in space: triangles do not cross, triangles have one mutual vertex, triangles have one mutual side and triangles are congruent. For the first type the cubature

formula application is possible. For the others it is not possible due to the singularity of the expressions being integrated. Let us note that the expression under integration in (5) can be represented as a sum of homogeneous functions. Let the function $f(\bar{x})$ be a homogeneous function if for any $\lambda > 0$

$$f(\lambda\bar{x}) = \lambda^k f(\bar{x}).$$

Let us illustrate the method of integration of homogeneous functions from [22] taking as an example the integral:

$$J_0 = \int_{S_1} \int_{S_2} \frac{dS_x dS_y}{|\bar{x} - \bar{y}|},$$

where S_1, S_2 are shown in Figure 1.

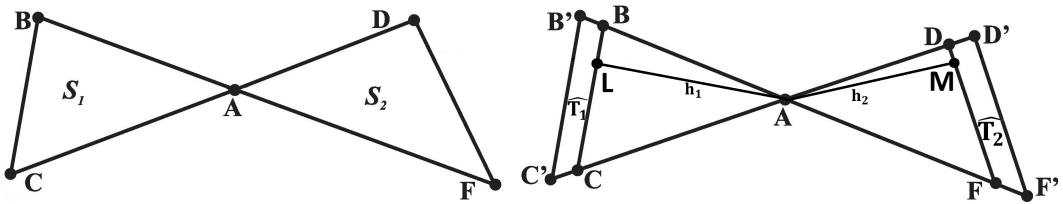


Figure 1. Illustration of homogeneous function integration by two triangles

Let \hat{S}_1 be a triangle $AB'C'$, obtained by stretching the triangle S_1 in λ times with respect to point A . Similarly \hat{S}_2 is a triangle $AD'F'$, obtained by stretching triangle S_2 in λ times with respect to point A . Let $J(\lambda)$ be

$$J(\lambda) = \int_{\hat{S}_1} \int_{\hat{S}_2} \frac{dS_x dS_y}{|\bar{x} - \bar{y}|}.$$

Substituting variables $\bar{x} = \lambda\bar{x}_1, \bar{y} = \lambda\bar{y}_1$ integral $J(\lambda)$ can be reduced to:

$$J(\lambda) = \lambda^3 \int_{S_1} \int_{S_2} \frac{dS_{x_1} dS_{y_1}}{|\bar{x}_1 - \bar{y}_1|}. \tag{6}$$

Let \hat{T}_1 be trapezium $B'BCC'$, \hat{T}_2 — trapezium $DD'F'F$. Let us calculate the limit of difference ratio:

$$\left. \frac{\partial J(\lambda)}{\partial \lambda} \right|_{\lambda=1} = \lim_{\lambda \rightarrow 1} \frac{(J(\lambda) - J(1))}{(\lambda - 1)}.$$

Using the additivity of integrals as a set function over which they are taken we have:

$$\left. \frac{\partial J(\lambda)}{\partial \lambda} \right|_{\lambda=1} = \lim_{\lambda \rightarrow 1} \frac{1}{\lambda - 1} \left[\left(\int_{\hat{T}_1} \int_{S_2} + \int_{\hat{S}_1} \int_{T_2} + \int_{\hat{T}_1} \int_{\hat{T}_2} \right) \frac{dS_{x_1} dS_{y_1}}{|\bar{x}_1 - \bar{y}_1|} \right]. \quad (7)$$

From (7) we have:

$$\left. \frac{\partial J(\lambda)}{\partial \lambda} \right|_{\lambda=1} = h_1 \int_{BC} \int_{S_2} \frac{dl_{x_1} dS_{y_1}}{|\bar{x}_1 - \bar{y}_1|} + h_2 \int_{S_1} \int_{DF} \frac{dS_{x_1} dl_{y_1}}{|\bar{x}_1 - \bar{y}_1|}, \quad (8)$$

where h_1 — height LA , h_2 — height AM . Differentiating (6) by λ and taking into account (8), we get:

$$J_0 = J(1) = \frac{1}{3} \left[h_1 \int_{BC} \int_{S_2} \frac{dl_{x_1} dS_{y_1}}{|\bar{x}_1 - \bar{y}_1|} + h_2 \int_{S_1} \int_{DF} \frac{dS_{x_1} dl_{y_1}}{|\bar{x}_1 - \bar{y}_1|} \right]. \quad (9)$$

It must be mentioned that the expressions on the right hand of (9) are regular integrals. It is possible to use the cubature formula for calculations of these integrals.

After application of this method all singular integrals from (5) can be reduced to the superposition of regular integrals of lower order, for calculation of which a cubature formula can be used. In the case when the triangles have one common side or coincide, this approach should be applied successively twice and three times respectively. The method of integration illustrated above allows to reduce all singular integrals from (5) to superpositions of regular integrals of lower order, the calculation of which can be done by cubature.

4. Iterative methods for nonlinear systems solving

In practice to achieve the demanded approximation accuracy it is necessary to split region G into smaller elements, that leads to huge dimension rise of the nonlinear discretized systems of the equations. It is extremely difficult to apply methods which require inversion of high order matrixes. So, for solving discretized systems of equations (4) simple iterative process is used:

$$[C] \hat{B}_{k+1} = (\hat{H}^S + ([A] + [C]) \hat{M}(\hat{B}_k)),$$

$$\hat{B}_0 = \bar{0}, \quad k = 1, 2, \dots$$

This process will be finished when equation residuals become less than the previously set value ε . For solving linear systems of equations $[C]\bar{x} = \bar{y}$ the incomplete Kholetsky expansion method in combination with the conjugate gradient method are used [23].

5. Magnet system modelling

The method of volume integral equations with the linear approximation of magnetization has been used for modelling the dipole and quadrupole magnets. The model of a variant of the projected dipole magnet for CBM experiment (GSI, Darmstadt) is shown In Figure 2a. A splitting of the magnet into the tetrahedrons has been done with the help of the generator **3DFEMMesh**. In the process of modelling the dipole symmetry of magnetic field has been taken into account, that allowed to reduce the number of unknown parameters by 8 times. One eighth of the magnet has been divided into 5264 tetrahedrons. There are 1363 vertexes in all tetrahedrons. In Figure 2b the distribution of the magnet field module inside the magnet is shown. The results given in Figure 2c show agreement of the present method with the famous code **TOSCA** [6] which is based on solving partial differential equations.

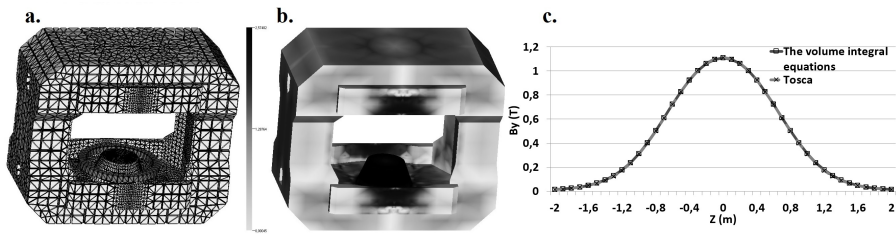


Figure 2. 3D modelling of dipole magnet CBM

The proposed approach has been also applied to the modelling of the **BOOSTER** quadrupole magnet of the projected accelerating complex **NICA** (JINR, Dubna).

In the process of modelling the quadrupole symmetry of magnetic field has been taken into account. This allowed to reduce the number of unknown parameters by 16 times. One sixteenth of the magnet was divided into 7040 tetrahedrons. The total number of vertexes was 1729. In Figure 3a there is a computer model of the magnet. In Figure 3b the allocation of magnet field module inside the magnet is shown. The resulting comparison obtained by the proposed method and **TOSCA** code is given in Figure 3c.

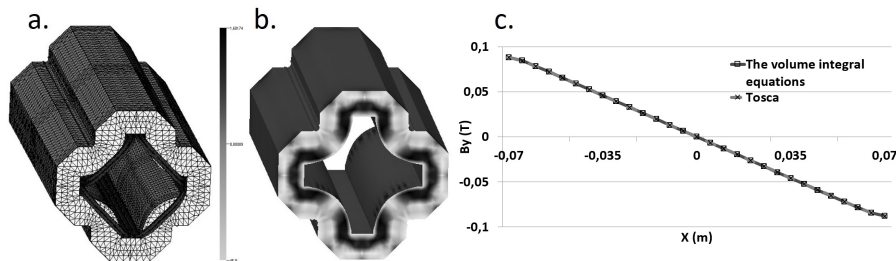


Figure 3. 3D modelling of quadrupole magnet BOOSTER

6. Conclusion

The issues of applying the volume integral equation method to the calculations of magnetic systems have been considered in this article. Within the framework of finite element method for discretization of continual equations an alternative approach has been used. This method is based on the substitution of observation points with integration by division elements. Thus, the main problem of applying the volume integral equation method which is related to kernel singularity is removed. The suggested approach allows to increase the order of approximation of the initial equations. Procedures for calculations of matrix coefficients for discretized equations and methods for solving a corresponding non-linear system of equations have been suggested. The results of magnet system simulations based on this approach are in agreement with the calculations by other programs.

References

1. C. W. Trowbridge, J. K. Sykulski, Some key developments in computational electromagnetics and their attribution, *IEEE transactions on magnetics* 42 (4) (2006) 503–508. doi:10.1109/TMAG.2006.872491.
2. A. G. Armstrong, *GFUN3D User Guide*. RL-76-029/A, CERN (1976).
3. A. A. Halacsy, Three-dimensional analysis of magnetic fields, in: *Proceedings 3rd International Conference on Magnet Technology*, Hamburg, 1970, pp. 113–128.
4. M. J. Friedman, Mathematical study of the nonlinear singular integral magnetic field equation I, *SIAM Journal on Applied Mathematics* 39 (1) (1980) 14–20. doi:10.1137/0139003.
5. M. J. Friedman, Mathematical study of the nonlinear singular integral magnetic field equation II, *SIAM Journal on Numerical Analysis* 18 (4) (1981) 644–653. doi:10.1137/0718042.
6. J. Simkin, C. W. Trowbridge, Three dimensional non-linear electromagnetic field computations using scalar potentials, *IEE Proceedings B – Electric Power Applications* 127 (6) (1990) 368–374. doi:10.1049/ip-b.1980.0052.
7. J. A. Stratton, *Electromagnetic theory*, McGraw-hill, 1941.
8. J. D. Jackson, *Classical electrodynamics*, 2nd Edition, John Wiley & Sons, 1975.
9. O. C. Zienkiewicz, *The finite element method in engineering science*, McGraw-hill, 1971.
10. J. T. Oden, *Finite elements of nonlinear continua*, McGraw-Hill, New York, 1971.
11. W. G. Strang, G. J. Fix, *An analysis of the finite element method*, Prentice-Hall, 1973.
12. J. P. Aubin, *Approximation of elliptic boundary-value problems*, Wiley-Interscience, 1972.
13. P. G. Akishin, A. A. Sapozhnikov, Linear approximation of volume integral equations for the problem of magnetostatics, in: *EPJ Web Conferences. Mathematical Modeling and Computational Physics (MMCP 2017)*, Vol. 173, 2018, Article Number 03001. doi:10.1051/epjconf/201817303001.

14. Z. Cendes, Magnetic field computation using Delaunay triangulation and complementary finite element methods, *IEEE Transactions on Magnetics* 19 (1983) 2551–2554. doi:10.1109/TMAG.1983.1062841.
15. E. K. Buratynski, A three-dimensional unstructured mesh generator for arbitrary internal boundaries, in: *Numerical Grid Generation in Computational Fluid Mechanics: Proceedings*, Pineridge Press, Swansea, 1988, pp. 621–631.
16. M. Berzins, Mesh quality: a function of geometry, error estimates or both?, *Engineering with Computers* 15 (1999) 236–247. doi:10.1007/s003660050019.
17. L. Durbeck, Evaporation: a technique for visualizing mesh quality, in: *8th International Meshing Roundtable*, Sandia National Laboratories, South Lake Tahoe, 1999, pp. 259–265.
18. P. G. Akishin, A. A. Sapozhnikov, Automatic generation of three-dimensional grids, *JINR*, Dubna, 2015.
URL [http://www1.jinr.ru/Preprints/2015/058\(P11-2015-58\).pdf](http://www1.jinr.ru/Preprints/2015/058(P11-2015-58).pdf)
19. P. G. Akishin, A. A. Sapozhnikov, 3DFEMMesh – program for automatic generation of three-dimensional Mesh.
URL <http://wwwinfo.jinr.ru/programs/jinrplib/3dfemmesh/indexe.html>
20. M. Abramowitz, I. Stegun, *Handbook of mathematical functions with functions, graphs, and mathematical tables*, 1964.
21. I. P. Mysovskikh, Interpolation cubature formulas [Interpolyatsionnyye kubaturnyye formuly], Nauka, Moscow, 1981, in Russian.
22. P. G. Akishin, The integral equation method in magnetostatic problems: abstract of a PhD thesis, Ph.D. thesis, *JINR*, Dubna, in Russian (1983).
23. J. A. Meijerink, H. A. van der Vorst, An iterative solution method for linear systems of which the coefficient matrix is a symmetric M -matrix, *Mathematics of Computation* 31 (137) (1977) 148–162. doi:10.2307/2005786.

For citation:

P. G. Akishin, A. A. Sapozhnikov, The volume integral equation method in magnetostatic problem, *Discrete and Continuous Models and Applied Computational Science* 27 (1) (2019) 60–69. DOI: 10.22363/2658-4670-2019-27-1-60-69.

Information about the authors:

Pavel G. Akishin (Russian Federation) — Doctor of Physical and Mathematical Sciences, Deputy Head of Scientific Department of Computational Physics, Laboratory of Information Technologies, Joint Institute for Nuclear Research (e-mail: akishin@jinr.ru, phone: +7(49621)62630, ORCID: <https://orcid.org/0000-0001-9542-046X>, ResearcherID: B-8330-2016, Scopus Author ID: 56780566600)

Andrey A. Sapozhnikov (Russian Federation) — Junior Researcher of Scientific Department of Computational Physics, Laboratory of Information Technologies, Joint Institute for Nuclear Research (e-mail: asap@jinr.ru, phone: +7(49621)62630, ORCID: <https://orcid.org/0000-0002-1270-043X>, Scopus Author ID: 57200759121)